nature portfolio

https://doi.org/10.1038/s41586-025-09666-9

# Supplementary information

# Oxidative potential of atmospheric particles in Europe and exposure scenarios

In the format provided by the authors and unedited

# Oxidative Potential of Atmospheric Particles in Europe and Exposure Scenarios

**Tassel et al.**

**Supplementary Information**

## S1. OP and health: epidemiological and toxicological evidence

We conducted a literature review on the link between OP and health, focusing more on recent literature (post 2019). We targeted publications using acellular OP data, in particular including AA or DTT tests. Before 2019, most epidemiological studies on OP and health concerned short-term exposure. The main tests included in the studies were the ascorbic acid (AA), dithiothreitol (DTT), glutathione (GSH) and electron spin resonance (ESR) tests, but the tests for which the greatest number of associations with health parameters were established were DTT and GSH assays. Several studies have shown associations with health outcomes for OP but not for PM mass, or that associations with OP were stronger than with PM mass. More recently, studies using 2,7-dichlorofluorescein (DCFH) assay or measuring OH radical formation, and some studies exploring the long-term effects of OP have been published (Borlaza, 2022; Marsal, 2023; Meng, 2023; Borlaza-Lacoste, 2024). These recent articles, along with others examining the short-term effects of OP (Tang, 2022; Marsal, 2024) or PM mass when OP is elevated (Weichenthal, 2021; Korsiak, 2022), provide growing evidence of the link between OP and health outcomes or biological pathways, both in the short and long term, as well as the relevance of this indicator as a complement to PM mass concentration.

**Supplementary Table 1. Review of recent literature on the link between OP and health**

| Reference | Year | Design of the study | Exposure window | Exposure parameter | Health outcome | Adjustment factors | Main results / conclusions for PM |
|---|---|---|---|---|---|---|---|
| Bates, J.T. et al. Reactive Oxygen Species Generation Linked to Sources of Atmospheric Particulate Matter and Cardiorespiratory Effects. *Environ. Sci. Technol*. **49**, 13605–13612. (2015). | 2015 | Time series analyses in Atlanta from Aug 1, 1998 to Dec 31, 2009 | Short term | Total $PM_{2.5}$ mass and $OP^{DTT}$ of WS-$PM_{2.5}$ (estimated for the period of 1998−2009 by MLR and CMB methods) | Cardiorespiratory outcomes: emergency department visits for asthma/wheezing and congestive heart failure | Temporal trends, temperature and humidity indicators, indicators of hospital contribution time periods, season of year, day of week, holiday indicators, interaction terms (season x max temperature, season x day of week) <u>Models</u>: single pollutant, two pollutants ($OP_v^{DTT}$ + $PM_{2.5}$ mass) | $OP_v^{DTT}$ was positively associated to the health outcomes in both single and two-pollutant models. $PM_{2.5}$ mass was not significantly associated with the outcomes. |
| Janssen, N.A.H. et al. Associations between three specific a-cellular measures of the oxidative potential of particulate matter and markers of acute airway and nasal inflammation in healthy volunteers. *Occup. Environ. Med*. **72**, 49–56. (2015). | 2015 | Semiexperimental study, RAPTES: 31 healthy young adults exposed for 5h to air pollution to at least 3 sites out of 5 (underground train station, traffic sites, farm, urban background) in the Netherlands from March to November 2009 | Short term | PM mass, $OP_v^{DTT}$, $OP_v^{ESR}$ and $OP_v^{AA}$ of $PM_{10}$ and $PM_{2.5}$ for a 5h exposure to ambient air pollution | $Fe_{NO}$, (IL)-6 in NAL, lung function, vascular inflammatory and coagulation parameters in blood 2h after exposure | Temperature, relative humidity, season, pollen and respiratory infections (only for $FE_{NO}$ and lung function), use of oral contraceptives (only for blood parameters except IL-6), endotoxin (only for NAL and serum IL-6) <u>Models</u>: single pollutant, two pollutants (OP + PM mass, PM composition, PNC, $NO_2$ or $O_3$) | The three OP were significantly associated with markers of airway and nasal inflammation, but not with other health endpoints. These associations were still significant after adjustment for co-pollutants only when the underground site was excluded. PM mass (both $PM_{2.5}$ and $PM_{10}$) was only significantly associated with NAL IL-6. |
| Fang, T. et al. Oxidative potential of ambient water-soluble $PM_{2.5}$ in the southeastern United States: Contrasts in sources and health associations between ascorbic acid (AA) and dithiothreitol (DTT) assays. *Atmospheric Chem. Phys*. **16**, 3865–3879. (2016). | 2016 | Time series analyses in Atlanta from Aug 1, 1998 to Dec 31, 2009 (Southeastern Center for Air Pollution & Epidemiology (SCAPE) study) | Short term | Daily $OP_v^{AA}$ and $OP_v^{DTT}$ of WS-$PM_{2.5}$ (estimated for the period 1998-2009 by PMF and CMB-E models) | Daily ED visits for respiratory diseases, including pneumonia, COPD, asthma and wheeze, and cardiovascular diseases, including IHD and CHF | Temporal trends, meteorological variables, indicators of hospital contribution time periods, season of year, day of week and holiday, and interaction terms (season x max temperature, season x day of week) <u>Models</u>: single pollutant | $OP_v^{DTT}$ was significantly positively associated to ED visits for both asthma or wheeze and CHF but not with COPD, IHD or pneumonia. $OP_v^{AA}$ was not significantly associated with any health outcome. |
| Maikawa, C.L. et al. Particulate Oxidative Burden as a Predictor of Exhaled Nitric Oxide in Children with Asthma. *Environ. Health Perspect*. **124**, 1616–1622. (2016). | 2016 | Panel study, 62 asthmatic school-aged children living in specific areas in Montreal near oil refineries | Short term | Daily $PM_{2.5}$ mass, $OP_m^{AA}$, $OP_v^{AA}$, $OP_m^{GSH}$ and $OP_v^{GSH}$ of $PM_{2.5}$ for 10 days | $Fe_{NO}$ | Temperature, sex, use of rescue medication, allergies <u>Models</u>: single pollutant, multi pollutants (OP or $PM_{2.5}$ mass + $O_3$) | $OP^{GSH}$ (both metrics) was positively associated with $Fe_{NO}$ in the previous 24h, and over 1-day lag and 2-day lag periods. $PM_{2.5}$ mass and $OP^{AA}$ were not positively associated with $Fe_{NO}$. Adjusting on ozone concentration did not change the results. |
| Weichenthal, S. et al. Oxidative burden of fine particulate air pollution and risk of cause-specific mortality in the Canadian Census Health and Environment Cohort (CanCHEC). *Environ. Res*. **146**, 92–99. (2016). | 2016 | Cohort, Canadian Census Health and Environment Cohort (CanCHEC): 193,300 people in Ontario (Canada) for the years 1998-2009 | Long term | Annual average $PM_{2.5}$ mass, $OP_v^{AA}$ and $OP_v^{GSH}$ of $PM_{2.5}$ from 30 provincial monitoring site across Ontario | Cause-specific mortality (all non-accidental causes, cardiometabolic diseases, IHD, respiratory diseases, lung cancers) in Ontario, Canada | Age, sex, aboriginal ancestry, visible minority status, immigrant status, marital status, highest level of education, employment status, occupational classification, and household income <u>Models</u>: single pollutant, two pollutants (OP + $PM_{2.5}$ mass) | $OP_v^{GSH}$ was associated with increased risk of non-accidental mortality, lung cancer and cardiometabolic mortality. $PM_{2.5}$ mass was associated with increased risk of non-accidental and lung cancer mortality. $OP_v^{GSH}$ was more strongly associated with lung cancer than $PM_{2.5}$ mass. $OP_v^{AA}$ was not significantly associated with any health outcome. $OP_v^{GSH}$ and $PM_{2.5}$ mass were still associated to lung cancers in the two-pollutant models with a greater magnitude for $OP_v^{GSH}$. $PM_{2.5}$ mass was still associated to non-accidental mortality |

| Reference | Year | Design of the study | Exposure window | Exposure parameter | Health outcome | Adjustment factors | Main results / conclusions for PM |
|---|---|---|---|---|---|---|---|
| | | | | | | | in the two-pollutant models, but not $OP_v^{GSH}$. |
| Yang, A. et al. Children's respiratory health and oxidative potential of PM2.5: the PIAMA birth cohort study. *Occup. Environ. Med.* **73**, 154–160. (2016). | 2016 | Prospective birth cohort, PIAMA: 3701 participants recruited during pregnancy in the Netherlands in 1996-1997 | Long term | Annual average $PM_{2.5}$ mass, $OP_v^{ESR}$, $OP_v^{DTT}$ and constituents of $PM_{2.5}$ and $NO_2$ at the home addresses (LUR) at birth and at the different follow-ups | Asthma and hay fever information collected annually until 8 years, at ages 11-12 and at 14 years, measurements of allergic sensitisation, lung function (spirometry) and $Fe_{NO}$ at 12 years | Sex, maternal education, parental allergies, breastfeeding, maternal smoking during pregnancy, smoking at home, use of gas for cooking, mould/dampness, pets at home, daycare attendance during first year of life and neighbourhood percentage of low-income households (+ age, height, weight, acute $NO_2$ effects and respiratory infections in the past 3 weeks for lung function and $Fe_{NO}$) <u>Models</u>: single pollutant, multi pollutants ($OP_v^{DTT}$ + $OP_v^{ESR}$, $PM_{2.5}$ mass, absorbance and constituents, $NO_2$) | $OP_v^{DTT}$ was positively associated with asthma incidence, prevalence of asthma symptoms and rhinitis, and negatively associated with $FEV_1$ and FVC. These associations were still found after adjustment for most co-pollutants, except for $NO_2$ with asthma endpoints and lung function. $PM_{2.5}$ mass and $OP_v^{ESR}$ were not significantly associated with respiratory health outcomes. |
| Abrams, J.Y. et al. Associations between Ambient Fine Particulate Oxidative Potential and Cardiorespiratory Emergency Department Visits. *Environ. Health Perspect.* **125**, 107008. (2017). | 2017 | Time series analyses: Atlanta (Georgia, US) during June 2012–April 2013 | Short term | Daily average $OP_v^{DTT}$ of WS-$PM_{2.5}$ | ED visits for asthma, COPD, pneumonia, URI, CHF, IHD, combined categories of respiratory diseases and cardiovascular diseases | Seasonal trends, weekdays, federal holidays, temperature, dew point, periods of hospital data contribution <u>Models</u>: single pollutant, two pollutants ($OP_v^{DTT}$+$PM_{2.5}$ mass and constituents, CO, $NO_2$, $O_3$, $SO_2$) | $OP_v^{DTT}$ was significantly associated with increased risk of ED visits for respiratory disease, asthma and IHD at lag 0-2. In the two-pollutant models, $OP_v^{DTT}$ was still associated with asthma ED visits and IHD, except when adjusting on $PM_{2.5}$ mass or OC (asthma) or CO (IHD). |
| Lavigne, É. et al. Fine Particulate Air Pollution and Adverse Birth Outcomes: Effect Modification by Regional Nonvolatile Oxidative Potential. *Environ. Health Perspect.* **126**, 077012. (2018). | 2018 | Retrospective cohort study conducted using 196,171 singleton births in 31 cities in Ontario (Canada) from 2006 to 2012 | Short and long term | $PM_{2.5}$ mass, $OP_v^{AA}$ and $OP_v^{GSH}$ of $PM_{2.5}$ during pregnancy | Preterm birth, term LBW, and term birth weight | Maternal age at delivery, marital status, maternal cigarette smoking during pregnancy, infant sex, parity, previous caesarean section delivery, maternal comorbidities, month and year of birth, gestational age, SES (+ gestational age for term LBW and term birth weight + temperature and humidity for preterm birth acute exposure) <u>Models</u>: single pollutant, two pollutants (OP or $PM_{2.5}$ mass + $NO_2$, $O_3$, $O_x$, $O_x^{wt}$) | $OP_v^{GSH}$ was more strongly associated to term LBW than $PM_{2.5}$ mass. The associations between $OP_v^{GSH}$ during the first trimester of pregnancy and term LBW was still significant after adjusting for $NO_2$ and $O_3$. Between-city differences in $OP_v^{GSH}$ modified the associations between $PM_{2.5}$ mass and term LBW or preterm birth. No influence on associations with $PM_{2.5}$ mass was observed for $OP_v^{AA}$. |
| Liu, L. et al. Metals and oxidative potential in urban particulate matter influence systemic inflammatory and neural biomarkers: A controlled exposure study. *Environ. Int.* **121**, 1331–1340. (2018). | 2018 | Single-blind randomized cross-over trial: 53 non-smoking volunteers exposed to concentrated ambient particles during 130 min in an exposure chamber | Short term | $OP_m^{AA}$, $OP_m^{GSH}$ and components of PM (coarse, fine and ultrafine CAP exposures) for a 130 min exposure to CAP | Biomarkers in blood and urine measured 1-hour and 21-hour post exposure | Age, sex, BMI, season, PM size, PM mass | $OP_m^{AA}$ and $OP_m^{GSH}$ were significantly associated with inflammatory and neural biomarkers. |
| Weichenthal, S. et al. Association of Sulfur, Transition Metals, and the Oxidative Potential of Outdoor $PM_{2.5}$ with Acute Cardiovascular Events: A | 2021 | National case-crossover study: 93,344 adult cases in Canada between 2016 and 2017 | Short term | Monthly $PM_{2.5}$ mass (+ S, metals, $OP_m^{AA}$, $OP_m^{GSH}$ and $OP_m^{DTT}$ of $PM_{2.5}$) | Acute cardiovascular events | Lag-0 mean temperature and $O_x^{wt}$ | $PM_{2.5}$ mass was more strongly associated with the outcomes in men when both metals and S concentrations were high. The same trend for $PM_{2.5}$ mass could be observed with both OP and S (for the 3 OP metrics), as well as with $OP_m^{GSH}$ or $OP_m^{DTT}$ |

| Reference | Year | Design of the study | Exposure window | Exposure parameter | Health outcome | Adjustment factors | Main results / conclusions for PM |
|---|---|---|---|---|---|---|---|
| Case-Crossover Study of Canadian Adults. *Health Perspect*. **129**, 107005. (2021). | | | | | | | alone. This suggests that OP may partially reflect the heterogeneity of the acute effects of $PM_{2.5}$ on cardiovascular health. |
| Zhang, Y-J. et al. Polycyclic aromatic hydrocarbon exposure, oxidative potential in dust, and their relationships to oxidative stress in human body: A case study in the indoor environment of Guangzhou, South China. *Environ. Int.* **149**, 106405 (2021). | 2021 | Cross-sectional study, 101 families in Guangzhou (South China) in 2018 | Short term | PAHs on indoor dust and indoor air samples (and then OH-PAHs in urine), $OP_v^{DTT}$ on indoor dust samples | Biomarkers of DNA oxidative damage: 8-OHdG in urine | / | OH-PAHs in urine were positively associated with 8-OHdG, especially for males. PAHs from dust samples were not significantly associated with 8-OHdG. A potential but not significant positive association between $OP_v^{DTT}$ of dusts and 8-OHdG was observed. |
| Borlaza, L.J.S. et al. Personal exposure to $PM_{2.5}$ oxidative potential and its association to birth outcomes. *J. Expo. Sci. Environ. Epidemiol*. (2022). | 2022 | Parent-child cohort, SEPAGES: 405 pregnant women in Grenoble area (France) | Long term | Personal prenatal $PM_{2.5}$ mass, and $OP_v^{AA}$ and $OP_v^{DTT}$ of $PM_{2.5}$ | Offspring weight, height, and head circumference at birth | Maternal age, parity, height, head circumference, weight and BMI before pregnancy, educational level, marital status, maternal smoking at any time during the pregnancy, gestational duration, child sex, and season of conception<br>Models: single pollutant, two pollutants (OP + $PM_{2.5}$ mass) | $PM_{2.5}$ mass and $OP_v^{DTT}$ were associated with reduced weight and height at birth. Stronger effects on birth weight were found for $OP_v^{DTT}$ than $PM_{2.5}$ mass. All associations found with birth weight and height were attenuated in two-pollutant models compared to single-pollutant models. Regarding height, this attenuation was less pronounced for $OP_v^{DTT}$ than for $PM_{2.5}$ mass. $OP_v^{AA}$ was not associated with any parameter. |
| Korsiak, J. et al. Air Pollution and Pediatric Respiratory Hospitalizations: Effect Modification by Particle Constituents and Oxidative Potential. *Am. J. Respir. Crit. Care Med*. **206**, 1370–1378. (2022). | 2022 | Time-stratified case-crossover study: 10,500 children in Canada hospitalized between June 2016 and December 2017 | Short term | Daily $PM_{2.5}$ mass and oxidant gases, and monthly $PM_{2.5}$ constituents, $OP_m^{AA}$, $OP_m^{GSH}$ and $OP_m^{DTT}$ | Respiratory hospitalizations | Lag-1 mean temperature and $O_x^{wt}$ | Overall, $PM_{2.5}$ mass was not associated with respiratory hospitalizations at lag-1. $PM_{2.5}$ mass was associated with respiratory hospitalizations when $OP_m^{GSH}$ or some metals concentrations were above the median. |
| Tang, Z. et al. The Oxidative Potential of Fine Particulate Matter and Biological Perturbations in Human Plasma and Saliva Metabolome. *Environ. Sci. Technol*. **56**(11), 7350–7361 (2022). | 2022 | Panel Study, Dorm Room Inhalation to Vehicle Emission (DRIVE) study: 54 non-smoking students living in one of 2 dormitories located near and far from a congested highway in Atlanta (US) | Short term | Indoor and outdoor $OP_m^{DTT}$ and $OP_v^{DTT}$ of WS-$PM_{2.5}$ and WI-$PM_{2.5}$ between September and January of 2015 | HRM profiling on 4 venous blood and 12 saliva samples | Dormitory, age, gender, BMI, race, moving days, time point | All OP metrics were associated with several metabolic pathways, especially leukotriene metabolism and galactose metabolism in plasma and vitamin E metabolism and leukotriene metabolism in saliva. OP metrics were directly associated with 5 metabolites. OP seems to be more biologically relevant than $PM_{2.5}$ mass in terms of oxidative stress and inflammation driven pathways. |
| Marsal, A. et al. Prenatal Exposure to PM2.5 Oxidative Potential and Lung Function in Infants and Preschool- Age Children: A Prospective Study. *Environ. Health Perspect*. **131**, 017004. (2023). | 2023 | Parent-child cohort, SEPAGES: 356 mother–child pairs in Grenoble area (France) | Long term | Personal prenatal $PM_{2.5}$ mass, and $OP_v^{AA}$ and $OP_v^{DTT}$ of $PM_{2.5}$ | Children lung function at 6 weeks (TBFVL and $N_2$MBW) and 3 years (AOS) | Child's height, weight, sex, age, season of sampling, breastfeeding, environmental tobacco smoke, maternal age and BMI before pregnancy, parental level of education, parental history of rhinitis, and mean temperature during pregnancy<br>Models: single pollutant, two pollutants (OP + $PM_{2.5}$ mass, $NO_2$) | Prenatal $OP_v^{DTT}$ was negatively associated with children FRC at 6 weeks. $PM_{2.5}$ mass showed similar but weaker tendency than $OP_v^{DTT}$ in the association with FRC. $OP_v^{DTT}$ tended to be positively associated with the frequency dependant resistance of the lungs at 3 years. Results for OP and FRC or $R_{rs7-19}$ remained similar when adjusting on $PM_{2.5}$ mass. |

| Reference | Year | Design of the study | Exposure window | Exposure parameter | Health outcome | Adjustment factors | Main results / conclusions for PM |
|---|---|---|---|---|---|---|---|
| Meng, Q. et al. Fine Particulate Matter Metal Composition, Oxidative Potential, and Adverse Birth Outcomes in Los Angeles. *Environ. Health Perspect.* **131**, 107012. (2023). | 2023 | Birth cohort: 285,614 singletons born in Los Angeles County (California) in the period 2017–2019 | Long term | $PM_{2.5}$ mass, metals, BC and ROS concentration, $OP_v^{OH}$ and $OP_v^{DTT}$ of $PM_{2.5}$, $NO_2$ during pregnancy | Risk of preterm birth and term LBW | Fetal sex, parity, maternal age, maternal race/ethnicity, maternal birthplace, payment source for prenatal care, maternal education, and maternal smoking<br>Models: single pollutant, two pollutants (OP + $PM_{2.5}$ mass, $NO_2$) | $PM_{2.5}$ mass, BC, Ba, Zn and $OP_v^{OH}$ were positively associated with preterm birth (still significant after adjustment on $NO_2$ but not after adjustment on $PM_{2.5}$ mass). $OP_v^{DTT}$ and Ba were positively associated with term LBW. The association found with $OP_v^{DTT}$ was almost not affected by the adjustment on $PM_{2.5}$ mass, unlike $NO_2$. ROS was positively associated with the 2 outcomes (still significant after adjustment on either $PM_{2.5}$ mass or $NO_2$ for term LBW but not for preterm birth). |
| Borlaza-Lacoste, L. et al. Oxidative potential of particulate matter and its association to respiratory health endpoints in high-altitude cities in Bolivia. *Environ. Res.* **255,** 119179. (2024). | 2024 | Time series analysis: La Paz et El Alto in Bolivia | Short term | $PM_{10}$ sources, $PM_{10}$ mass and $OP_v^{DTT}$ and $OP_v^{DCFH}$ of $PM_{10}$ between April 2016 and June 2017<br>$PM_{2.5}$ mass, and BC concentration, $OP_v^{DTT}$ and $OP_v^{DCFH}$ of $PM_{2.5}$ between June 2017 and June 2018 | Weekly numbers of hospital visits for pneumonia, ARI others than pneumonia during the PM sampling period | Time trend, temperature, relative humidity, wind speed, and with a random effect representing the city<br>Models: single pollutant, multipollutant (OP + PM mass, the other OP metric) | $PM_{2.5}$: PM mass and $OP_v^{DTT}$ were positively associated with ARI at a 2-wks lag. $OP_v^{DTT}$ was also positively associated with ARI at lag 0, and tended to be associated with ARI and pneumonia at lag 1. $OP_v^{DCFH}$ and BC were not associated with the health outcomes.<br>$PM_{10}$: PM mass and $OP_v^{DTT}$ were sometimes negatively associated with pneumonia. Positive associations were found between pneumonia and traffic from gasoline-powered vehicles, as well as between ARI and dust. Some sources were negatively associated with some outcomes.<br>Little difference was observed for multipollutant models compared to unipollutant models. |
| Marsal, A. et al. Effects of personal exposure to the oxidative potential of PM2.5 on oxidative stress biomarkers in pregnant women. *Sci. Total Environ.* **911**, 168475. (2024). | 2024 | Parent-child cohort, SEPAGES: 300 pregnant women in Grenoble area (France) | Short term | Personal prenatal $PM_{2.5}$ mass, and $OP_v^{AA}$, $OP_v^{DTT}$, $OP_m^{AA}$ and $OP_m^{DTT}$ of $PM_{2.5}$ | Three biomarkers of oxidative stress: 8-OHdG, MDA, 8-isoPGF2α | Educational level, history of rhinitis and asthma, age, BMI, parity, active or passive smoking, temperature, gestational age, number of samples in the pool, storage time at -80°C before analysis<br>Models: single pollutant | $OP_m^{AA}$ was positively associated with 8-OHdG, with stronger effects at low $PM_{2.5}$ mass. $PM_{2.5}$ mass was not associated with the biomarkers of oxidative stress. |
| **Reviews** | | | | | | | |
| Bates, J.T. et al. Review of Acellular Assays of Ambient Particulate Matter Oxidative Potential: Methods and Relationships with Composition, Sources, and Health Effects. *Environ. Sci. Technol.* **53**, 4003-4019. (2019). | 2019 | Review on OP drivers and epidemiological evidence of its relevance for future health analyses | Review | / | / | / | Epidemiological studies showing positive associations between OP and respiratory health end points: 7 with $OP^{DTT}$, 2 with $OP^{ESR}$, 2 with $OP^{GSH}$ and 1 with $OP^{AA}$. Epidemiological studies showing positive associations between OP and cardiovascular health end points: 4 with $OP^{DTT}$ and 1 with $OP^{GSH}$. Associations with health end points were stronger for OP than PM mass in some of these studies. |
| Øvrevik, J. Oxidative Potential Versus Biological Effects: A Review on the Relevance of Cell- | 2019 | Review on cell-free/abiotic OP assays and the relevance of OP as exposure | Review | / | / | / | Some epidemiological have found correlations between OP and biological effects, while others reported no association. Links have been found |

| Reference | Year | Design of the study | Exposure window | Exposure parameter | Health outcome | Adjustment factors | Main results / conclusions for PM |
|---|---|---|---|---|---|---|---|
| Free/Abiotic Assays as Predictors of Toxicity from Airborne Particulate Matter. *Int. J. Mol. Sci.* **20**, 4772. (2019). | | metric in epidemiological studies. | | | | | between OP and redox responses (intracellular ROS, oxidative damage and antioxidant responses in vitro), but not with other biological effects (inflammation, non-oxidative DNA-damage, etc.). $OP^{DTT}$ have been associated to asthma/wheeze in humans. |
| Gao, D., Ripley, S., Weichenthal, S., Pollitt, K.J.G. Ambient particulate matter oxidative potential: Chemical determinants, associated health effects, and strategies for risk management. *Free Radic. Biol. Med.* **151**, 7–25. (2020). | 2020 | Review on acellular OP techniques, PM chemical constituents driving OP response and epidemiologic literature on associations between OP and health | Review | / | / | / | There is some epidemiological evidence of the relevance of OP in health studies, especially $OP^{DTT}$ and $OP^{GSH}$ which showed significant associations with acute and chronic cardiorespiratory outcomes. Some studies showed stronger associations with $OP^{DTT}$ than with $PM_{2.5}$ mass. Some studies highlighted the capacity of $OP^{GSH}$ to modify the relationship between $PM_{2.5}$ mass and cardiorespiratory outcomes. |
| He, L. & Zhang, J. Particulate matter (PM) oxidative potential: Measurement methods and links to PM physicochemical characteristics and health effects. *Crit. Rev. Environ. Sci. Technol.* **53**(2), 177–197 (2023). | 2023 | Review on OP techniques, OP physical and chemical drivers and epidemiological and toxicological evidence of its relevance for future health analyses | Review | / | / | / | Cellular OP assays seem to better assess the biological effects of PM than acellular OP tests. There is some evidence of a link between OP and cardiovascular and respiratory diseases for short-term exposure, supporting the use of OP as a more health-relevant indicator than concentration, but few associations have been demonstrated for long-term exposure or for other health effects. OP still faces methodological issues. |

[WS-PM: Water-soluble PM; WI-PM: Water-insoluble PM; MLR: Multivariate linear regression; CMB: Chemical mass balance; $Fe_{NO}$: Fractional exhaled nitric oxide; (IL)-6: Interleukin-6; NAL: Nasal lavage; CMB-E: chemical mass balance method with ensemble-averaged source impact profiles; ED: emergency department; COPD: chronic obstructive pulmonary disease; IHD: ischemic heart failure; CHF: congestive heart failure; LUR: land-use regression; $FEV_1$: forced expiratory volume (1s); FVC: forced vital capacity; $FEF_{25-75}$: forced expiratory flow at 25-75% of vital capacity; PEF: peak expiratory flow; PNC: particle number concentration; URI: upper respiratory infection; LBW: low birth weight; $O_x$: combined oxidant capacity of $NO_2$ and $O_3$ calculated as their sum; $O_x^{wt}$: redox-weighted oxidant capacity of $NO_2$ and $O_3$ calculated as a weighted average using redox potentials as the weights; CAP: concentrated ambient particle; TBFVL: tidal breathing analysis; $N_2$MBW: nitrogen multiple-breath washout; AOS: airwave oscillometry; FRC: functional residual capacity; ARI: acute respiratory infections; 8-OHdG: 8-hydroxy-2-deoxyguanosine; MDA: malondialdehyde;; 8-isoPGF2α: 8-iso-prostaglandin-F2α; OH-PAHs: hydroxyl PAHs; HRM: High-Resolution Metabolomic.]

## S2. OP and PM mass averages in Europe

*OP and PM variability*. Coefficients of variation (CV) per site for $PM_{10}$ samples fluctuate between 46% and 128% for $OP_v^{AA}$, between 36% and 106% for $OP_v^{DTT}$ and between 26% and 78% for $PM_{10}$ mass. For all $PM_{10}$ data together, the CV are 116% for $OP_v^{AA}$, 85% for $OP_v^{DTT}$ and 65% for $PM_{10}$ mass. For $PM_{2.5}$ data, CV per site ranges from 56% to 133% for $OP_v^{AA}$, from 49% to 111% for $OP_v^{DTT}$ and from 38% to 134% for $PM_{2.5}$ mass. This is consistent with Salana et al (2024) regarding $PM_{2.5}$ mass (CV between 30% and 80%) and $OP_v^{DTT}$ (CV between 50% and 100%). $OP_v^{AA}$ has a higher variability than that of $OP_v^{DTT}$ and PM mass, which are quite similar.

**Supplementary Table 2. $OP_v$ and $OP_m$ values for both AA and DTT assays and PM mass concentration for the 43 European stations and the 5 types of sites (11,436 samples).**

| Parameter mean ± SD | PM size | $OP_m$ (nmol $min^{-1}.\mu g^{-1}$) | | $OP_v$ (nmol $min^{-1}$ $m^{-3}$) | | PM mass (µg $m^{-3}$) | N[a] |
|---|---|---|---|---|---|---|---|
| | | **AA** | **DTT** | **AA** | **DTT** | | |
| **Total data[b,c]** | | | | | | | |
| | $PM_{10}$ | 0.078 ± 0.038 | 0.088 ± 0.027 | 1.5 ± 0.73 | 1.7 ± 0.65 | 20.1 ± 5.1 | 8,126 |
| | $PM_{2.5}$ | 0.071 ± 0.026 | 0.074± 0.020 | 1.1 ± 0.77 | 1,0 ± 0.49 | 14.1 ± 6.8 | 2,797 |
| | $PM_1$ | 0.052 ± 0.020 | 0.061 ± 0.018 | 0.60 ± 0.22 | 0.78 ± 0.30 | 14.4 ± 4.3 | 513 |
| **Grouped by location[b,c]** | | | | | | | |
| BERN | $PM_{10}$ | 0.2 ± 0.04 | 0.14 ± 0.03 | 3.71 ± 1.71 | 2.69 ± 1.45 | 19.42 ± 10.22 | 738 |
| STG-Cle | $PM_{10}$ | 0.1 ± 0.04 | 0.13 ± 0.05 | 2.54 ± 3.26 | 2.65 ± 2.09 | 27.87 ± 14.58 | 147 |
| RBX | $PM_{10}$ | 0.08 ± 0.04 | 0.1 ± 0.03 | 2.07 ± 1.41 | 2.71 ± 1.71 | 27.8 ± 15.26 | 159 |
| BOSSONS | $PM_{10}$ | 0.15 ± 0.07 | 0.1 ± 0.02 | 2.15 ± 1.34 | 1.51 ± 0.66 | 14.67 ± 7.19 | 96 |
| ZURICH | $PM_{10}$ | 0.12 ± 0.05 | 0.13 ± 0.05 | 2.03 ± 1.53 | 2.4 ± 2.1 | 18.38 ± 12.57 | 204 |
| BCN | $PM_{10}$ | 0.07 ± 0.03 | 0.11 ± 0.04 | 1.56 ± 0.88 | 2.48 ± 1.15 | 23.31 ± 8.94 | 270 |
| LENS | $PM_{10}$ | 0.05 ± 0.03 | 0.09 ± 0.03 | 1.02 ± 1.13 | 1.74 ± 1.46 | 25.86 ± 14.74 | 116 |
| ROUEN | $PM_{10}$ | 0.06 ± 0.05 | 0.09 ± 0.03 | 1.46 ± 1.49 | 2.26 ± 1.19 | 25.39 ± 13.88 | 135 |
| NOGENT | $PM_{10}$ | 0.08 ± 0.04 | 0.09 ± 0.04 | 2.07 ± 2.3 | 2.24 ± 1.83 | 24.88 ± 13.72 | 199 |
| CHAM | $PM_{10}$ | 0.11 ± 0.06 | 0.14 ± 0.03 | 2.3 ± 2.69 | 2.33 ± 1.56 | 23.47 ± 12.72 | 98 |
| NICE | $PM_{10}$ | 0.06 ± 0.03 | 0.14 ± 0.04 | 0.99 ± 0.62 | 2.24 ± 0.8 | 22.88 ± 7.72 | 110 |
| PARIS-lh | $PM_{10}$ | 0.07 ± 0.04 | 0.09 ± 0.02 | 1.41 ± 1.01 | 1.79 ± 1.06 | 20.74 ± 13.22 | 386 |
| TAL | $PM_{10}$ | 0.06 ± 0.04 | 0.1 ± 0.03 | 1.17 ± 1.25 | 1.64 ± 1.25 | 20.05 ± 10.98 | 235 |
| PARIS-lcpp | $PM_{10}$ | 0.08 ± 0.04 | 0.12 ± 0.06 | 1.52 ± 1.22 | 2.29 ± 1.51 | 19.4 ± 9.26 | 184 |
| LYON | $PM_{10}$ | 0.08 ± 0.04 | 0.08 ± 0.03 | 1.5 ± 1.3 | 1.64 ± 1.33 | 19.32 ± 12.19 | 122 |
| GRE-fr | $PM_{10}$ | 0.08 ± 0.05 | 0.09 ± 0.04 | 1.53 ± 1.58 | 1.62 ± 1.33 | 18.9 ± 10.23 | 1,351 |
| MRS-lcp | $PM_{10}$ | 0.06 ± 0.04 | 0.1 ± 0.04 | 1.04 ± 0.8 | 1.78 ± 0.97 | 18.62 ± 8.09 | 271 |
| AIX | $PM_{10}$ | 0.06 ± 0.04 | 0.07 ± 0.03 | 1.76 ± 1.75 | 1.96 ± 1.29 | 18.39 ± 10.21 | 59 |
| GRE-cb | $PM_{10}$ | 0.08 ± 0.05 | 0.09 ± 0.04 | 1.48 ± 1.32 | 1.59 ± 1.06 | 18.08 ± 9.39 | 247 |
| ATH | $PM_{10}$ | 0.06 ± 0.05 | 0.08 ± 0.02 | 2.2 ± 2.65 | 2.44 ± 1.24 | 31.99 ± 14.89 | 147 |
| RDAM | $PM_{10}$ | 0.06 ± 0.03 | 0.08 ± 0.02 | 1.43 ± 0.71 | 1.89 ± 0.71 | 16.21 ± 4.17 | 56 |
| KRAK | $PM_{10}$ | 0.05 ± 0.01 | 0.07 ± 0.02 | 1.48 ± 1.19 | 2.04 ± 1.26 | 28.69 ± 18.9 | 63 |
| GSY | $PM_{10}$ | 0.04 ± 0.03 | 0.06 ± 0.04 | 1.05 ± 0.86 | 1.63 ± 1.54 | 27.05 ± 14.6 | 133 |
| FSM | $PM_{10}$ | 0.06 ± 0.05 | 0.05 ± 0.02 | 1.13 ± 0.84 | 1.1 ± 0.7 | 21.89 ± 7.84 | 29 |
| PDB | $PM_{10}$ | 0.07 ± 0.04 | 0.08 ± 0.03 | 0.59 ± 0.5 | 1.63 ± 0.87 | 20.74 ± 7.05 | 139 |
| CALAIS | $PM_{10}$ | 0.03 ± 0.02 | 0.1 ± 0.04 | 1.42 ± 1.07 | 1.67 ± 1.13 | 20.5 ± 9.21 | 139 |
| LHV | $PM_{10}$ | 0.08 ± 0.05 | 0.07 ± 0.03 | 1.17 ± 0.96 | 1.06 ± 0.57 | 15.33 ± 7.37 | 136 |
| KANAL | $PM_{10}$ | 0.15 ± 0.12 | 0.09 ± 0.05 | 2.64 ± 3.36 | 1.52 ± 1.62 | 15.62 ± 11.65 | 120 |
| BASEL | $PM_{10}$ | 0.09 ± 0.05 | 0.06 ± 0.02 | 1.24 ± 1.09 | 0.79 ± 0.55 | 13.97 ± 9.26 | 90 |
| PASSY | $PM_{10}$ | 0.12 ± 0.1 | 0.12 ± 0.07 | 3.02 ± 3.79 | 3.19 ± 2.25 | 29.19 ± 18.4 | 437 |
| VIF | $PM_{10}$ | 0.08 ± 0.06 | 0.08 ± 0.04 | 1.27 ± 1.52 | 1.12 ± 0.8 | 14.32 ± 9.34 | 253 |
| MGD | $PM_{10}$ | 0.1 ± 0.06 | 0.09 ± 0.05 | 1.78 ± 1.92 | 1.61 ± 1.42 | 16.7 ± 10.6 | 240 |
| PAYRN | $PM_{10}$ | 0.06 ± 0.03 | 0.07 ± 0.03 | 0.71 ± 0.49 | 0.92 ± 0.73 | 13.49 ± 8.31 | 103 |
| MSY | $PM_{10}$ | 0.04 ± 0.03 | 0.05 ± 0.02 | 0.41 ± 0.25 | 0.55 ± 0.38 | 12.82 ± 6.24 | 106 |
| ARREST | $PM_{10}$ | 0.07 ± 0.05 | 0.04 ± 0.02 | 1.4 ± 1.38 | 0.91 ± 0.67 | 18.58 ± 8.89 | 140 |
| MARNAZ | $PM_{10}$ | 0.09 ± 0.06 | 0.12 ± 0.03 | 1.57 ± 2.02 | 1.77 ± 1.18 | 18.49 ± 12.28 | 93 |
| DIEPPE | $PM_{10}$ | 0.03 ± 0.02 | 0.04 ± 0.03 | 0.54 ± 0.53 | 0.72 ± 0.63 | 16.72 ± 8.3 | 137 |
| PLOURZ | $PM_{10}$ | 0.02 ± 0.06 | 0.06 ± 0.02 | 0.23 ± 0.22 | 0.88 ± 0.53 | 15.73 ± 8.13 | 171 |
| OPE | $PM_{10}$ | 0.05 ± 0.06 | 0.07 ± 0.06 | 0.4 ± 0.47 | 0.6 ± 0.4 | 9.54 ± 6.54 | 200 |
| COURMAY | $PM_{10}$ | 0.05 ± 0.04 | 0.07 ± 0.04 | 0.55 ± 0.4 | 1 ± 0.83 | 17.58 ± 12.9 | 67 |
| BERN | $PM_{2.5}$ | 0.11 ± 0.03 | 0.1 ± 0.02 | 1.35 ± 0.75 | 1.27 ± 0.74 | 12.61 ± 7.52 | 644 |
| SRJV | $PM_{2.5}$ | 0.07 ± 0.05 | 0.05 ± 0.02 | 2.96 ± 3.43 | 1.75 ± 1.5 | 32.69 ± 22.95 | 103 |
| ZURICH | $PM_{2.5}$ | 0.08 ± 0.04 | 0.08 ± 0.02 | 0.82 ± 0.56 | 0.83 ± 0.56 | 10.8 ± 6.97 | 90 |
| BCN | $PM_{2.5}$ | 0.05 ± 0.03 | 0.07 ± 0.02 | 0.89 ± 0.54 | 1.2 ± 0.59 | 17.48 ± 6.32 | 197 |
| PARIS-lcpp | $PM_{2.5}$ | 0.06 ± 0.04 | 0.08 ± 0.04 | 0.85 ± 0.79 | 1.02 ± 0.84 | 12.51 ± 7.26 | 69 |
| LILLE | $PM_{2.5}$ | 0.07 ± 0.06 | 0.09 ± 0.03 | 0.68 ± 0.67 | 0.86 ± 0.49 | 11.19 ± 6.82 | 121 |
| PARIS-lh | $PM_{2.5}$ | 0.07 ± 0.04 | 0.08 ± 0.03 | 0.73 ± 0.58 | 0.8 ± 0.55 | 10.48 ± 6.27 | 806 |
| ATH | $PM_{2.5}$ | 0.08 ± 0.05 | 0.08 ± 0.03 | 1.94 ± 2.22 | 1.92 ± 1.2 | 24.7 ± 16.61 | 152 |
| BDP | $PM_{2.5}$ | 0.13 ± 0.07 | 0.12 ± 0.06 | 2.09 ± 1.98 | 1.8 ± 1.23 | 15.03 ± 8.69 | 61 |
| BASEL | $PM_{2.5}$ | 0.06 ± 0.05 | 0.06 ± 0.02 | 0.68 ± 0.86 | 0.62 ± 0.57 | 10.6 ± 7.76 | 90 |
| MGD | $PM_{2.5}$ | 0.09 ± 0.07 | 0.08 ± 0.04 | 1.13 ± 1.45 | 0.88 ± 0.86 | 10.61 ± 7.2 | 153 |
| PAYRN | $PM_{2.5}$ | 0.04 ± 0.03 | 0.06 ± 0.03 | 0.39 ± 0.34 | 0.61 ± 0.48 | 9.68 ± 6.73 | 102 |
| MSY | $PM_{2.5}$ | 0.05 ± 0.06 | 0.05 ± 0.04 | 0.34 ± 0.22 | 0.44 ± 0.3 | 9.62 ± 4.68 | 107 |
| OPE | $PM_{2.5}$ | 0.03 ± 0.02 | 0.05 ± 0.03 | 0.23 ± 0.22 | 0.5 ± 0.54 | 8.79 ± 7.16 | 102 |
| BCN | $PM_1$ | 0.05 ± 0.03 | 0.06 ± 0.02 | 0.66 ± 0.33 | 0.87 ± 0.41 | 14.71 ± 4.91 | 94 |
| MRS-lcp | $PM_1$ | 0.08 ± 0.07 | 0.09 ± 0.07 | 0.76 ± 0.77 | 0.87 ± 0.76 | 13.65 ± 13.48 | 262 |
| KRAK | $PM_1$ | 0.04 ± 0.02 | 0.06 ± 0.01 | 0.71 ± 0.69 | 1.03 ± 0.85 | 19.73 ± 17.28 | 63 |
| MSY | $PM_1$ | 0.04 ± 0.04 | 0.04 ± 0.02 | 0.28 ± 0.17 | 0.35 ± 0.2 | 9.35 ± 4.39 | 94 |
| **Grouped by site type[b,d]** | | | | | | | |
| Traffic | $PM_{10}$ | 0.13 ± 0.03 | 0.12 ± 0.01 | 2.62 ± 0.38 | 2.39 ± 0.29 | 22.44 ± 3.26 | 1,140 |
| Urban | $PM_{10}$ | 0.07 ± 0.0 | 0.1 ± 0.0 | 1.56 ± 0.09 | 2.02 ± 0.07 | 21.93 ± 0.99 | 4,243 |
| Industrial | $PM_{10}$ | 0.07 ± 0.02 | 0.07 ± 0.01 | 1.33 ± 0.28 | 1.43 ± 0.11 | 20.22 ± 1.78 | 696 |
| Suburban | $PM_{10}$ | 0.12 ± 0.03 | 0.09 ± 0.02 | 1.85 ± 0.59 | 1.68 ± 0.73 | 18.86 ± 4.72 | 695 |
| Rural | $PM_{10}$ | 0.06 ± 0.01 | 0.07 ± 0.01 | 0.84 ± 0.19 | 1.0 ± 0.14 | 15.52 ± 1.0 | 1,252 |
| Traffic | $PM_{2.5}$ | 0.11 | 0.1 | 1.35 | 1.27 | 12.61 | 644 |
| Urban | $PM_{2.5}$ | 0.08 ± 0.01 | 0.08 ± 0.01 | 1.38 ± 0.3 | 1.28 ± 0.17 | 16.32 ± 2.42 | 1,634 |
| Suburban | $PM_{2.5}$ | 0.06 | 0.06 | 0.68 | 0.62 | 10.6 | 90 |
| Rural | $PM_{2.5}$ | 0.05 ± 0.01 | 0.06 ± 0.01 | 0.52 ± 0.21 | 0.61 ± 0.10 | 9.73 ± 0.33 | 463 |
| Urban | $PM_1$ | 0.01 ± 0.02 | 0.07 ± 0.01 | 0.71 ± 0.03 | 0.92 ± 0.05 | 16.03 ± 1.88 | 414 |
| Rural | $PM_1$ | 0.04 | 0.04 | 0.28 | 0.36 | 9.35 | 93 |

[a] Number of OP analysed samples.
[b] Weighted means with different weights depending on the season and equivalent weight for each site calculated with the DescrStatsW() function of the statsmodels package in Python (see Methods).
[c] Standard deviations calculated with the DescrStatsW() function of the statsmodels package in Python.
[d] Standard error of the mean (SEM) calculated with the DescrStatsW() function of the statsmodels package in Python if more than one site included in this site type.

## S3. Intrinsic OP and PM mass depending on site type

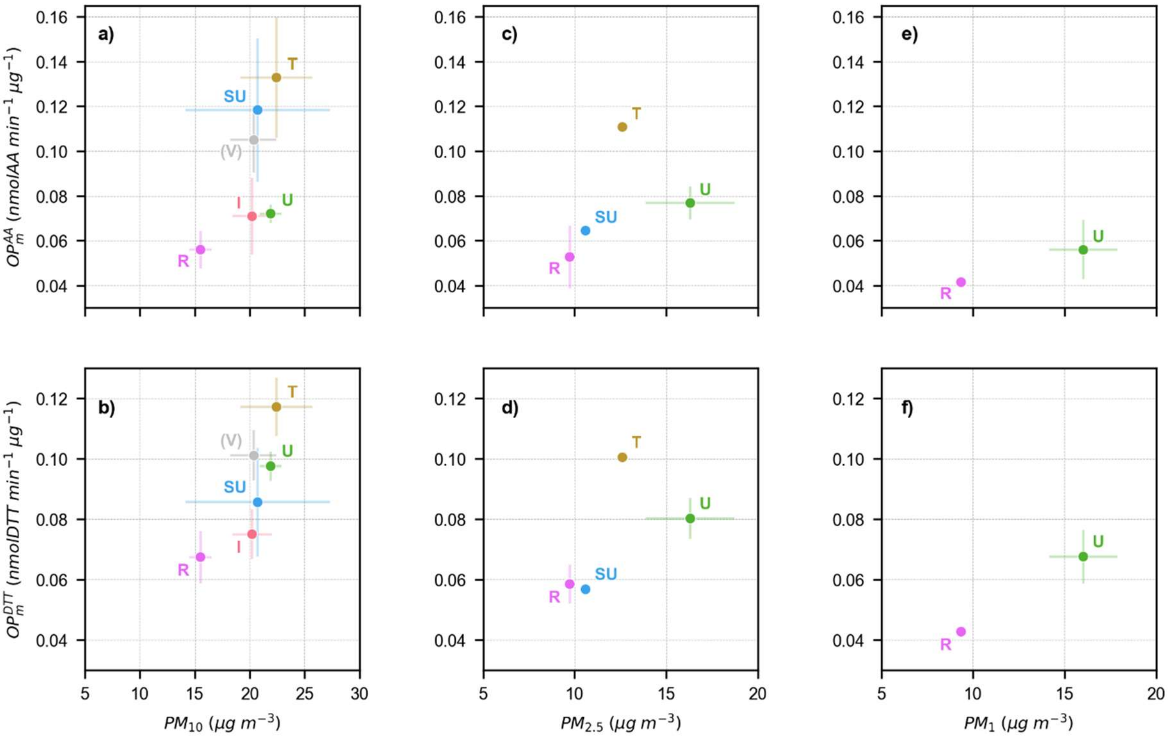


**Supplementary Figure 1| Mean $OP_m$ as a function of PM mass at different site types.** Mean values and corresponding standard errors of the mean (SEM). **(a)** $OP_m^{AA}$ and $PM_{10}$ mass concentration. **(b)** $OP_m^{DTT}$ and $PM_{10}$ mass concentration. **(c)** $OP_m^{AA}$ and $PM_{2.5}$ mass concentration. **(d)** $OP_m^{DTT}$ and $PM_{2.5}$ mass concentration. **(e)** $OP_m^{AA}$ and $PM_1$ mass concentration. **(f)** $OP_m^{DTT}$ and $PM_1$ mass concentration. T: Traffic (4 stations for $PM_{10}$, 1 station for $PM_{2.5}$), U: Urban (20 stations for $PM_{10}$, 8 stations for $PM_{2.5}$ and 3 stations for $PM_1$), I: Industrial (6 stations for $PM_{10}$), SU: Suburban (3 stations for $PM_{10}$, 1 station for $PM_{2.5}$), R: Rural (9 stations for $PM_{10}$, 4 stations for $PM_{2.5}$ and 1 station for $PM_1$), V: Valley (9 stations for $PM_{10}$). The mean for all sites with a valley topography has been added in grey for information purposes on the $PM_{10}$ graphs. The dots correspond to weighted means with weights depending on the season (see Methods section) and with equivalent weights for all sites within each site type. These weighted means were calculated with the DescrStatsW() function of the statsmodels package in Python. The error bars correspond to standard errors of the means of groups by site type.

## S4. Statistical tests

**Supplementary Table 3. Results from ANOVA tests testing the influence of the PM size fraction on $OP_v$, $OP_m$ and PM mass**

| Parameter | Sum of squares (SS) | Degrees of freedom (Df) | Mean squares (MS) | F statistic value | p-value |
|---|---|---|---|---|---|
| $OP_m^{AA}$ | 0.704886 | 2 | 0.352443 | 81.0750 | < 0.001 |
| $OP_m^{DTT}$ | 0.768336 | 2 | 0.384168 | 199.543 | < 0.001 |
| $OP_v^{AA}$ | 1779.14 | 2 | 889.570 | 239.714 | < 0.001 |
| $OP_v^{DTT}$ | 1835.18 | 2 | 917.590 | 472.753 | < 0.001 |
| PM mass | 121352 | 2 | 60676.0 | 408.868 | < 0.001 |

[Type 2 ANOVA tests were performed using anova_lm and ols functions of the statsmodels package in Python. N=11,436 samples]

**Supplementary Table 4. Results from ANOVA tests testing the influence of the site type on $OP_v$, $OP_m$ and PM mass across PM sizes**

| PM size fraction | Parameter | Sum of squares (SS) | Degrees of freedom (Df) | Mean squares (MS) | F statistic value | p-value |
|---|---|---|---|---|---|---|
| $PM_{10}$ | $OP_m^{AA}$ | 11.1921 | 4 | 2.79803 | 750.032 | < 0.001 |
| | $OP_m^{DTT}$ | 2.39671 | 4 | 0.599178 | 321.082 | < 0.001 |
| | $OP_v^{AA}$ | 6293.35 | 4 | 1573.34 | 409.951 | < 0.001 |
| | $OP_v^{DTT}$ | 2051.15 | 4 | 512.788 | 233.329 | < 0.001 |
| | PM mass | 59321.5 | 4 | 14830.4 | 95.2151 | < 0.001 |
| $PM_{2.5}$ | $OP_m^{AA}$ | 0.926622 | 3 | 0.463311 | 144.361 | < 0.001 |
| | $OP_m^{DTT}$ | 0.495618 | 3 | 0.247809 | 166.174 | < 0.001 |
| | $OP_v^{AA}$ | 190.672 | 3 | 95.3360 | 37.4727 | < 0.001 |
| | $OP_v^{DTT}$ | 142.607 | 3 | 71.3035 | 66.0368 | < 0.001 |
| | PM mass | 9543.26 | 3 | 4771.63 | 30.4781 | < 0.001 |
| $PM_1$ | $OP_m^{AA}$ | 0.023774 | 1 | 0.023774 | 8.26997 | < 0.001 |
| | $OP_m^{DTT}$ | 0.061994 | 1 | 0.061994 | 26.4532 | < 0.001 |
| | $OP_v^{AA}$ | 13.4125 | 1 | 13.4125 | 36.0913 | 0,004 |
| | $OP_v^{DTT}$ | 23.5836 | 1 | 23.5836 | 56.2103 | < 0.001 |
| | PM mass | 2994.88 | 1 | 2994.88 | 21.6701 | < 0.001 |

[Type 2 ANOVA tests were performed using anova_lm and ols functions of the statsmodels package in Python. N=11,436 samples (8,126 $PM_{10}$ samples; 2,797 $PM_{2.5}$ samples; 513 $PM_1$ samples)]

**Supplementary Table 5. p-values from t-tests on mean PM mass and $OP_m$ (AA and DTT) by site, comparing types of sites 2-by-2, for $PM_{10}$ size fraction**

| Parameter p-value (t-value) | Site type | Traffic | Urban | Industrial | Suburban | Rural |
|---|---|---|---|---|---|---|
| $PM_{10}$ mass | Traffic | - | - | - | - | - |
| | Urban | 0.835 (0.21) | - | - | - | - |
| | Industrial | 0.527 (0.66) | 0.400 (0.86) | - | - | - |
| | Suburban | 0.802 (0.26) | 0.720 (0.36) | 0.925 (-0.10) | - | - |
| | Rural | 0.021 (2.70) ** | < 0.001 (4.06) ** | 0.028 (2.47) ** | 0.207 (1.35) | - |
| $OP_m^{AA}$ | Traffic | - | - | - | - | - |
| | Urban | < 0.001 (4.20) ** | - | - | - | - |
| | Industrial | 0.074 (2.05) * | 0.921 (0.10) | - | - | - |
| | Suburban | 0.742 (0.35) | 0.006 (-3.06) ** | 0.189 (-1.45) | - | - |
| | Rural | 0.004 (3.61) ** | 0.062 (1.95) * | 0.403 (0.87) | 0.019 (2.79) ** | - |
| $OP_m^{DTT}$ | Traffic | - | - | - | - | - |
| | Urban | 0.095 (1.75) * | - | - | - | - |
| | Industrial | 0.011 (3.30) ** | 0.028 (2.35) ** | - | - | - |
| | Suburban | 0.155 (1.67) | 0.391 (0.88) | 0.549 (-0.63) | - | - |
| | Rural | 0.006 (3.40) ** | 0.003 (3.30) ** | 0.557 (0.60) | 0.338 (1.01) | - |

[**: p-values ≤ 0.05; *: p-values ≤ 0.1. N=40 sites. Degrees of freedom (df) for each comparison are as follows: Traffic-Urban, df=20; Traffic-Industrial, df=8; Traffic-Suburban, df=5; Traffic-Rural, df=11; Urban-Industrial, df=22; Urban-Suburban, df=19; Urban-Rural, df=25; Industrial-Suburban, df=7; Industrial-Rural, df=13; Suburban-Rural, df=10.]

## S5. Seasonality of $OP_m$

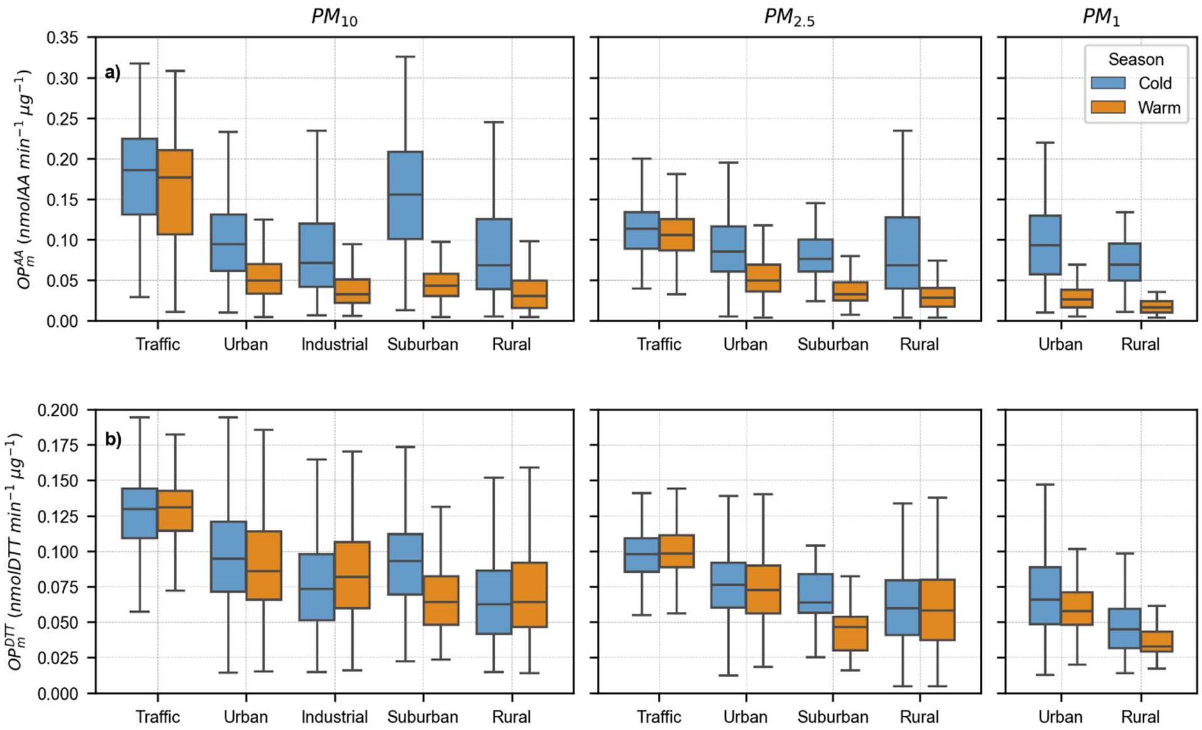


**Supplementary Figure 2| Box plot representations of seasonal means of a) $OP_m^{AA}$ and b) $OP_m^{DTT}$ for the cold (N-D-J-F-M) and warm (M-J-J-A-S) period at different PM fractions and site types.** The data exclude 1% of extreme values in each site type. N=9,342 samples.

## S6. $OP_v$ exposure scenarios

The sites with lowest $OP_v^{DTT}$ levels are MSY (Montseny, Spain) for both $PM_{10}$ and $PM_{2.5}$ in rural areas and GRE-cb (Grenoble hypercenter, France) for $PM_{10}$ and PARIS-lh (Paris, France) for $PM_{2.5}$ in urban stations. The rural stations with the highest $OP_v^{DTT}$ average value are PAYRN (Payerne, Switzerland) for both $PM_{10}$ and $PM_{2.5}$. Regarding $OP_v^{AA}$, the rural sites with the lowest levels are PLOURZ (Plouarzel, France) for $PM_{10}$ and OPE ("*Observatoire Pérenne de l'Environnement*", France) for $PM_{2.5}$, and the one with the highest levels for both size fractions (excluding Arrest which is too high in comparison with the order of magnitude of other rural sites and is not consistent with the intermediate scenario) is PAYRN (Payerne, Switzerland). The least polluted urban sites in terms of $OP_v^{AA}$ are NICE (Nice, France) for $PM_{10}$ and LILLE (Lille, France) for $PM_{2.5}$.

For comparison, if we used the same methodology to define $PM_{10}$ mass exposure scenarios, we would have $PM_{10}$ mass reference values between 9.54 (OPE, France) and 18.6 µg $m^{-3}$ (Arrest, France). Concerning $PM_{2.5}$, the $PM_{2.5}$ mass reference values would vary between 8.79 (OPE, France) and 10.5 µg $m^{-3}$ (Paris Les Halles, France). The sites with the lowest pollution levels in rural and urban areas are not the same depending on the indicator chosen (PM mass, $OP_v^{AA}$ or $OP_v^{DTT}$). In addition, it is interesting to note that the WHO annual AQG for $PM_{10}$ (15 µg $m^{-3}$) is included in the range of $PM_{10}$ mass reference values obtained with this methodology and is very close to the mean $PM_{10}$ mass observed in rural areas ("low anthropogenic pollution" scenario). In the case of $PM_{2.5}$, even in the least polluted rural sites in the database, no site was found with mean $PM_{2.5}$ mass below or equal to the WHO annual AQG for $PM_{2.5}$ (5 µg $m^{-3}$), in agreement with a large-scale study of the rural sites in France (Font et al., 2024). However, for this latter size fraction, the regulatory annual threshold for $PM_{2.5}$ (10 µg $m^{-3}$) is very close to the $PM_{2.5}$ mass reference values that can be obtained with scenarios 2 and 3 in the methodology described here.

**Supplementary Table 6. Description of the $OP_v^{AA}$ exposure scenarios selected for each PM fraction.**

| OP exposure scenarios | | Description of OP exposure scenarios | PM size | $OP_{ref}$ [a] |
|---|---|---|---|---|
| 1 | Low urbanization scenario | Mean $OP_v$ level in the urban station with the lowest $OP_v$ level; i.e. NICE for $PM_{10}$ and LILLE for $PM_{2.5}$ | $PM_{10}$ | 0.99 |
| | | | $PM_{2.5}$ | 0.68 |
| 2 | Intermediate scenario | Mean $OP_v$ level in the rural station with the highest $OP_v$ level (except for ARREST in $PM_{10}$ [b]); i.e. PAYRN for both $PM_{10}$ and $PM_{2.5}$ | $PM_{10}$ | 0.71 |
| | | | $PM_{2.5}$ | 0.39 |
| 3 | Low anthropogenic pollution scenario | Mean $OP_v$ level in all rural areas | $PM_{10}$ | 0.60 |
| | | | $PM_{2.5}$ | 0.32 |
| 4 | Very low anthropogenic pollution scenario | Mean $OP_v$ level in the rural station with the lowest $OP_v$ level; i.e. PLOURZ for $PM_{10}$ and OPE for $PM_{2.5}$ | $PM_{10}$ | 0.23 |
| | | | $PM_{2.5}$ | 0.23 |

[a] $OP_{ref}$: $OP_v^{AA}$ reference value (nmol $min^{-1}$ $m^{-3}$)

[b] Mean $OP_v^{AA}$ in ARREST is too high in comparison with the order of magnitude of other rural sites and is not consistent with the intermediate scenario.

## S7. Long term trends

Throughout Europe, $PM_{10}$ mass has decreased substantially over recent decades, primarily due to reduced emissions of secondary inorganic aerosol (SIA) precursors. However, many other emission sources have either remained stable or increased—particularly those associated with high OP, such as non-exhaust traffic emissions and residential biomass burning (Borlaza et al., 2022). To investigate the implications for particle reactivity, we conducted an OP trend analysis at three representative sites: a rural background (OPE, France), an urban valley environment (Grenoble, France), and a traffic-impacted site (Bern, Switzerland). At the rural and traffic sites, $PM_{10}$ mass has decreased over the years, while $OP_v^{DTT}$ decreased less markedly—or even increased—indicating a relative increase in $OP_m^{DTT}$. In contrast, in the urban valley setting, $OP_v^{DTT}$ declined more than $PM_{10}$, suggesting different source dynamics. This results in substantial variability in $OP_m^{DTT}$ trends across environments. These trends likely reflect shifts in dominant sources (Ngoc Thuy Dinh et al., 2025). In valley sites, $OP_v^{DTT}$ correlates well with biomass burning markers such as levoglucosan (Extended Data Table 4), whereas in traffic environments, metallic tracers like Cu and Sb suggest a stronger influence of non-exhaust emissions. Thus, the relatively stable $OP_v^{DTT}$ and $OP_m^{DTT}$ values may result from sustained non-exhaust traffic emissions, while biomass burning and other emission sources have declined substantially. Importantly, targeting biomass burning alongside traffic would also reduce key toxic species like benzo(a)pyrene, a regulated carcinogen (Belis et al., 2011).

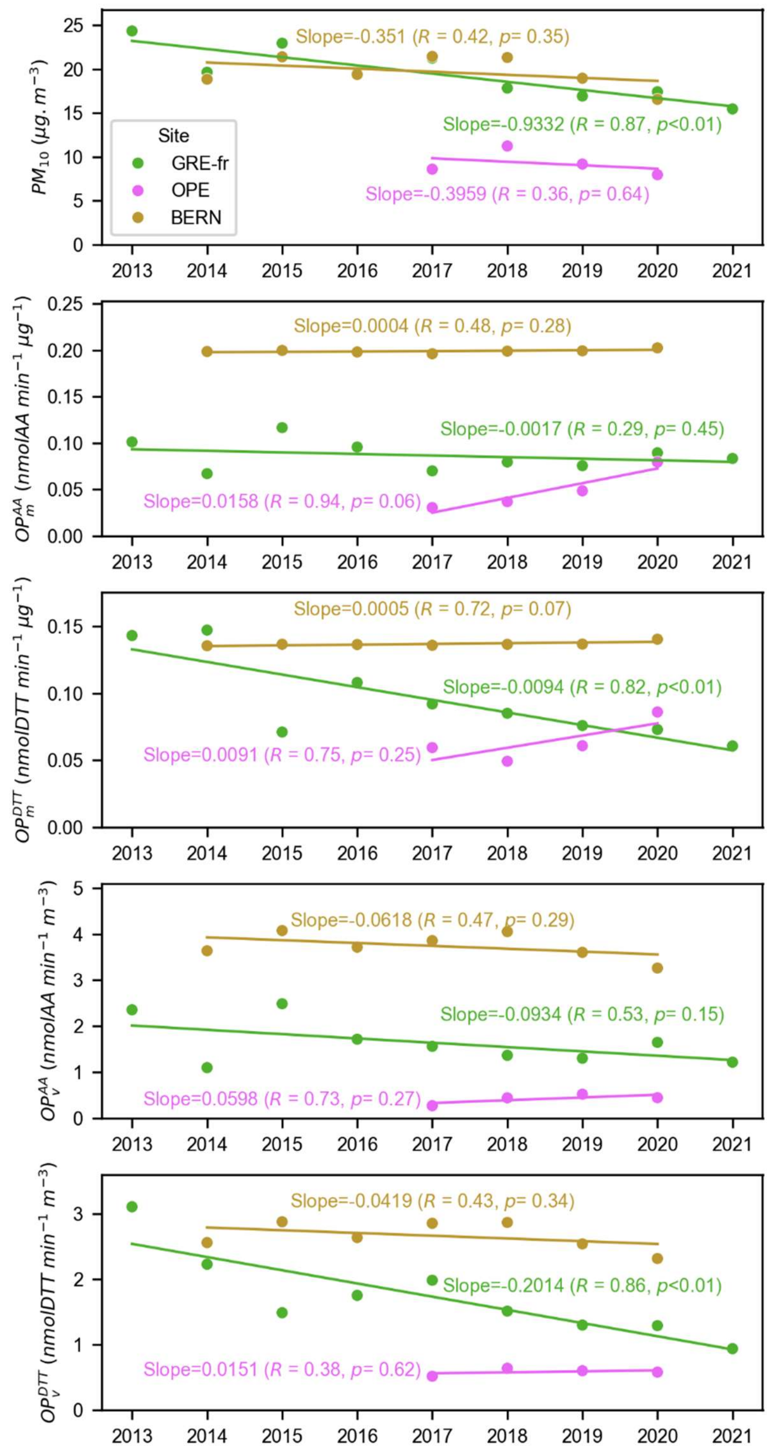


**Supplementary Figure 3| Yearly average levels of $PM_{10}$ mass concentration, $OP_m^{AA}$, $OP_m^{DTT}$, $OP_v^{AA}$ and $OP_v^{DTT}$ in OPE (France), GRE-fr (France) and BERN (Switzerland).** N=2,280. The dots correspond to weighted means with weights depending on the season (see Methods). The weighted means and the standard deviations were calculated with the DescrStatsW() function of the Statsmodels package in Python. The straights lines represent ordinary least squares linear regressions on yearly averages, performed with the statsmodels package in python. Data gathered 200 $PM_{10}$ samples collected between June 2017 and December 2020 for OPE (France); 726 $PM_{10}$ samples collected between January 2014 and December 2020 for Bern (Switzerland); and 1,354 $PM_{10}$ samples between January 2013 and May 2022.

## S8. Emission reduction matrix

*PM source apportionment.* In order to calculate all matrices, a source apportionment (SA) method was performed using positive matrix factorization (PMF). The methodology of the PMF with all the selected parameters has been described in detail in Weber et al. (2019) and Glojek et al. (2024). Briefly, by integrating time series measurements of $PM_{10}$ mass concentration and a large number of chemical tracers, this technique produced chemical profiles for each source and their contributions to $PM_{10}$. The measured data and their uncertainties (calculated from the analyses' uncertainties) formed the input matrix for the PMF model, implemented using EPA PMF 5.0 (Norris et al., 2014). The PMF was performed using a harmonized approach, which is following the recommendation of European commission (Belis et al., 2019) for selecting the input, validating the results and applying the constraint. The optimal solution has been determined notably by checking (1) the outlier's effect to the solution (less than 30% data outliers); (2) the clarity of the chemical profiles; (3) the contribution factors (contribution > 1% to the total $PM_{10}$ mass); (4) the distribution of the residuals (between -3 and 3); and (5) the correlation between measured and predicted concentrations (correlation coefficient > 0.5). The constraints were applied to the optimal solution which allow to limit errors caused by co-emissions from certain sources and reduce the uncertainty of the rotational ambiguity (Belis et al., 2019). The stability of the solutions is assessed using two methods: bootstrapping (correlation between the base run and boot runs > 0.6) and displacement (no significant rotational ambiguity in the constrained solution).

*OP source apportionment*. The OP SA basically performed using the Multiple Linear Regression analysis (MLR) where $OP_v$ is the dependent variable and PMF-derived sources are the independent variables (Eq.4).

$$OP_v = \sum_p^{i=1} OP_m^i * PM^i + e \qquad (4)$$

Where $OP_v$ is the observed volumetric OP (nmol min$^{-1}$ m$^{-3}$), $p$ is the number of PMF-derived $PM_{10}$ sources, $OP_m^i$ is the regression slope, denoted as the intrinsic OP of source i (nmol min$^{-1}$ µg$^{-1}$), $PM^i$ is the contribution of source i to $PM_{10}$ calculated using PMF (µg m$^{-3}$) and $e$ is the residual of the regression technique (nmol min$^{-1}$ m$^{-3}$).

The OP SA in Borlaza et al. (2022) and Glojek et al. (2024) were performed using the weighted least square techniques which are reported elsewhere in Bates et al. (2015) and Weber et al. (2019). In these SA, weightings were introduced to account for analytical uncertainty (higher uncertainty has less influence in the MLR model). On the other hand, another method has been developed in Dinh Ngoc Thuy et al. (2024) which selects the MLR techniques based on the characteristics of PMF-derived sources and $OP_v$. Eleven MLR techniques were tested to find the most appropriate model for each urban French site. For the 3 studies, the MLR models were performed 500 iterations runs, by randomly training on 80% of the dataset and validating on the remaining 20%, to ensure the robustness of the results. All the validation metrics for PMF and MLR can be found in the three studies.

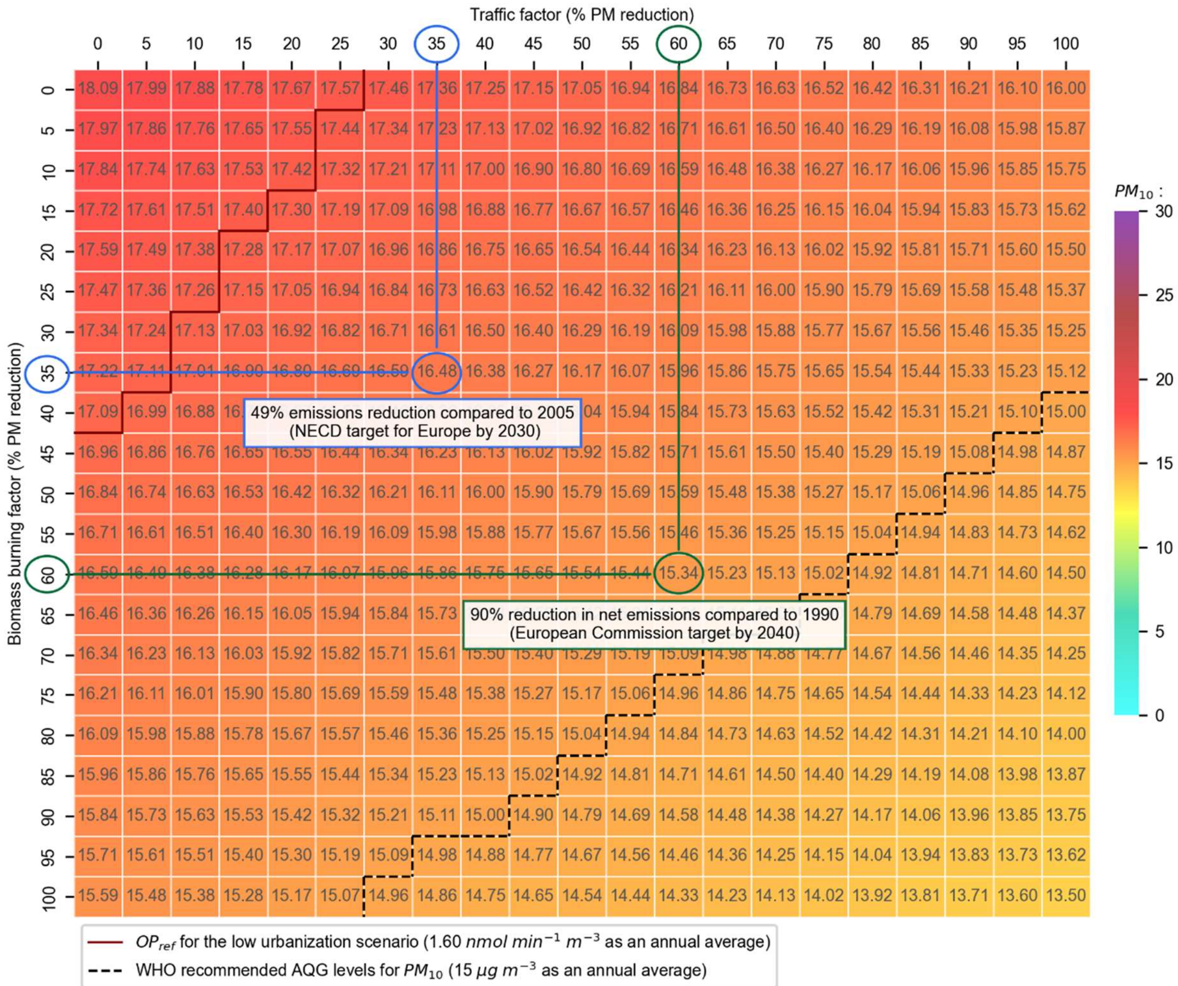


**Supplementary Figure 4| Matrix of $PM_{10}$ mass values based on the reduction of $PM_{10}$ from two sources (traffic and biomass burning factors) in four European urban sites (Grenoble, Talence, Nice and Barcelona).** The percentage reductions in traffic- and biomass-burning-related $PM_{10}$ refer to a multi-site, multi-year reference level based on average source contributions across the four studied sites (2012–2023). Data gathered 551 samples collected between March 2012 and April 2013 for Talence, between February 2017 and March 2018 for Grenoble, between July 2014 and May 2015 for Nice and between March 2022 and March 2023 for Barcelona. The matrix was calculated using PMF results from Dinh Ngoc Thuy et al. (2024). The solid line represents $OP_v^{DTT}$ reference value for the "low urbanization" scenario. $OP_v^{DTT}$ reference values for the other scenarios (≤ 0.92 nmolDTT $min^{-1}$ $m^{-3}$) are not shown because they are out of scale. The dashed line represents the WHO Air Quality Guidelines (AQG) level for $PM_{10}$ as an annual mean. The new regulatory threshold for $PM_{10}$ (20 µg $m^{-3}$) is not shown because it has already been reached in average for these four sites. The blue circle represents the $PM_{10}$ mass value that could be reached by a 35% reduction in $PM_{10}$ mass from the two sources (based on the $PM_{2.5}$ emission reduction target for Europe by 2030 set by the National Emission reduction Commitments Directive (NECD)[45]). The green circle represents the $PM_{10}$ mass value that could be reached by a 60% reduction in $PM_{10}$ mass from these two sources (based on the European Commission target for Europe by 2040). These two projected values correspond to the remaining reduction required to meet the EU targets from a 2012–2022 reference, based on emission inventories (see Methods section). The $PM_{10}$ mass levels (µg $m^{-3}$) are going from low to high values with the colours changing from blue to violet.

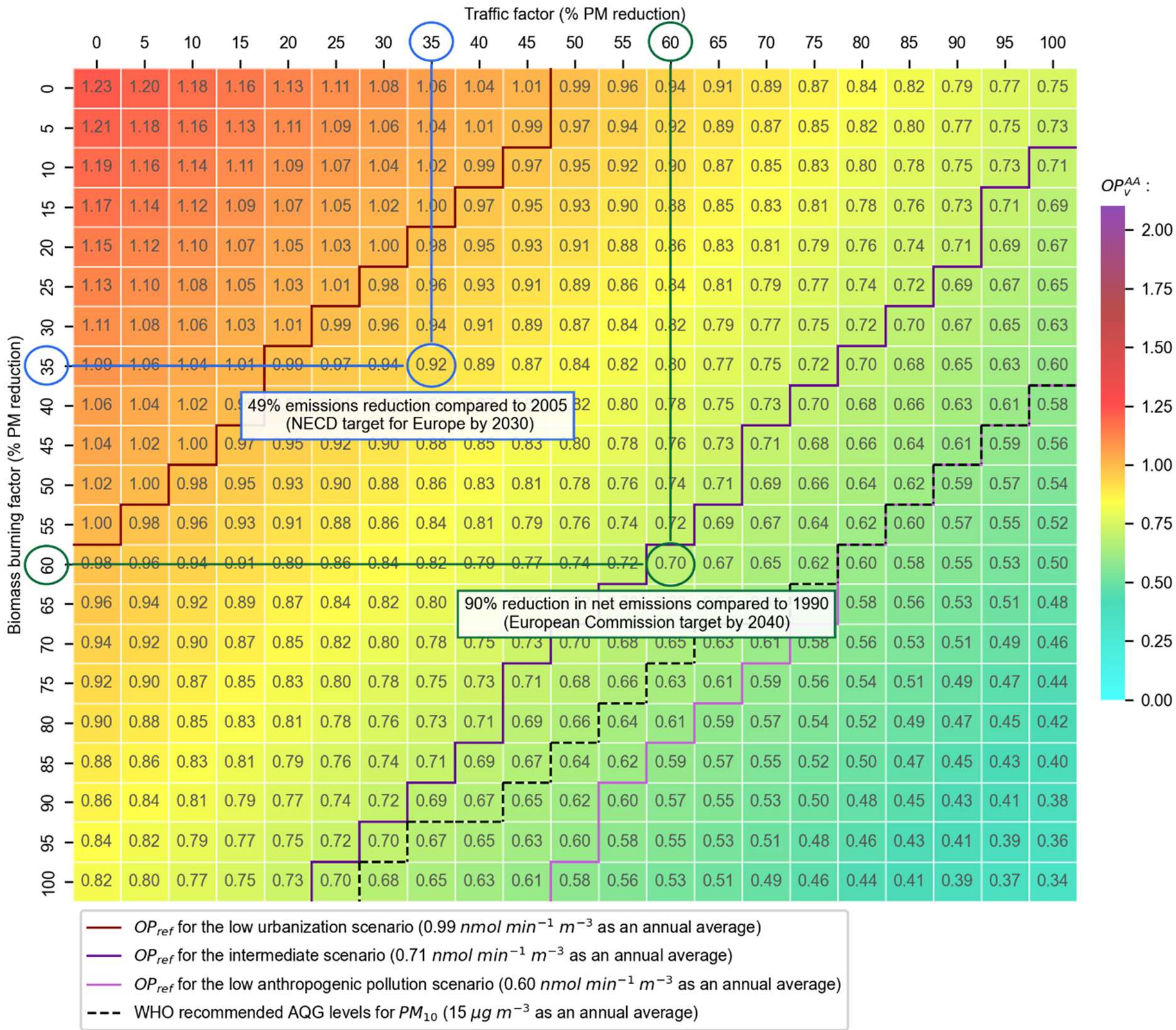


**Supplementary Figure 5| Matrix of $OP_v^{AA}$ values based on the reduction of $PM_{10}$ mass from two sources (traffic and biomass burning factors) in four European urban sites (Grenoble, Talence, Nice and Barcelona).** The percentage reductions in traffic- and biomass-burning-related $PM_{10}$ refer to a multi-site, multi-year reference level based on average source contributions across the four studied sites (2012–2023). Data gathered 551 samples collected in Talence, Grenoble, Nice and Barcelona between March 2012 and February 2023. The matrix was calculated using PMF and MLR results from Dinh Ngoc Thuy et al. (2024). The solid lines represent $OP_v^{AA}$ reference values for the "low urbanization" scenario, the "intermediate" scenario and the "low anthropogenic pollution" scenario. $OP_v^{AA}$ reference value for the "very low anthropogenic pollution" scenario (0.23 nmolAA $min^{-1}$ $m^{-3}$) is not shown because it is out of scale. The dashed line represents the WHO Air Quality Guidelines (AQG) level for $PM_{10}$ mass as an annual mean. This limit for $PM_{10}$ mass WHO target was drawn using a similar matrix with mean $PM_{10}$ mass values (Supplementary Fig. 4). The new regulatory threshold for $PM_{10}$ mass (20 µg $m^{-3}$) is not shown because it has already been reached in average for these four sites. The blue circle represents the $OP_v^{AA}$ value that could be reached by a 35% reduction in $PM_{10}$ mass from the two sources (based on the $PM_{2.5}$ emission reduction target for Europe by 2030 set by the National Emission reduction Commitments Directive (NECD)[45]). The green circle represents the $OP_v^{AA}$ value that could be reached by a 60% reduction in $PM_{10}$ mass from these two sources (based on the European Commission target for Europe by 2040). These two projected values correspond to the remaining reduction required to meet the EU targets from a 2012–2022 reference, based on emission inventories (see Methods section). The $OP_v^{AA}$ levels (nmolAA $min^{-1}$ $m^{-3}$) are going from low to high values with the colours changing from blue to violet.

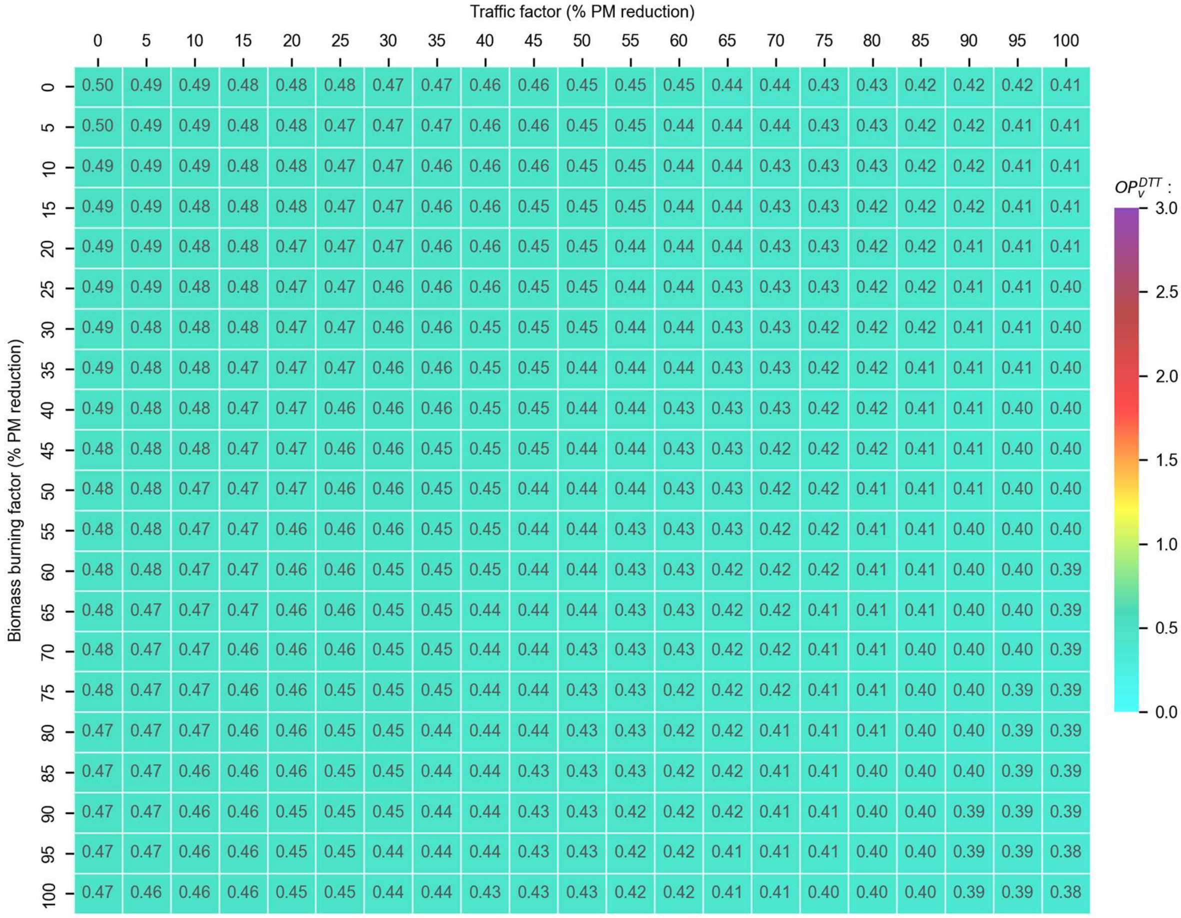


**Supplementary Figure 6| Matrix of $OP_v^{DTT}$ values based on the reduction of $PM_{10}$ from two sources (traffic and biomass burning factors) in the rural site of OPE ("Observatoire Pérenne de l'Environnement", France).** The percentage reductions in traffic- and biomass-burning-related $PM_{10}$ refer to a multi-year reference level based on average source contributions in OPE (2012–2020). Data gathered 438 samples collected between March 2012 and December 2020. The matrix was calculated using PMF and MLR results from Borlaza et al. (2022). The WHO Air Quality Guidelines (AQG) level and the new regulatory threshold for $PM_{10}$ (respectively 15 and 20 µg $m^{-3}$) are not shown because they have already been reached in average for this site. Similarly, all $OP_v^{DTT}$ reference values have been achieved. The $OP_v^{DTT}$ levels (nmolDTT $min^{-1}$ $m^{-3}$) are going from low to high values with the colours changing from blue to violet.

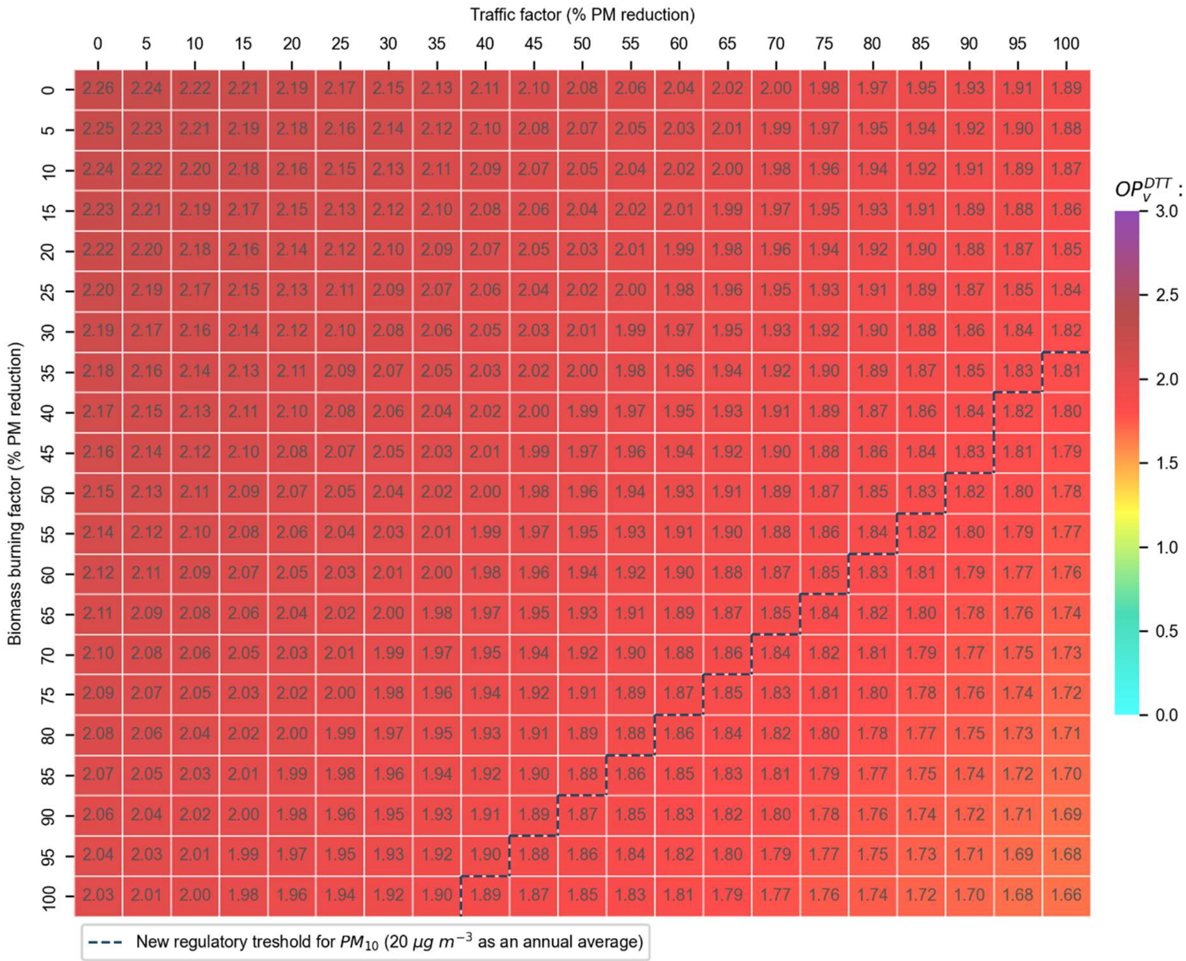


**Supplementary Figure 7| Matrix of $OP_v^{DTT}$ values based on the reduction of $PM_{10}$ from two sources (traffic and biomass burning factors) in the traffic site of RBX (Roubaix, France).** The percentage reductions in traffic- and biomass-burning-related $PM_{10}$ refer to a one-year reference level based on average source contributions in Roubaix (2013–2014). Data gathered 156 samples collected between January 2013 and May 2014. The matrix was calculated using PMF and MLR results from Dinh Ngoc Thuy et al. (2024). The dashed line represents the new regulatory $PM_{10}$ threshold as an annual mean. The WHO Air Quality Guidelines (AQG) level for $PM_{10}$ (15 µg $m^{-3}$) is not shown because it cannot be reached in average for this site only with the reduction of these two sources (out of scale). Similarly, all $OP_v^{DTT}$ reference values, even for the “low urbanization” scenario (1.60 nmolDTT $min^{-1}$ $m^{-3}$), are not shown because they are out of scale. The $OP_v^{DTT}$ levels (nmolDTT $min^{-1}$ $m^{-3}$) are going from low to high values with the colours changing from blue to violet.

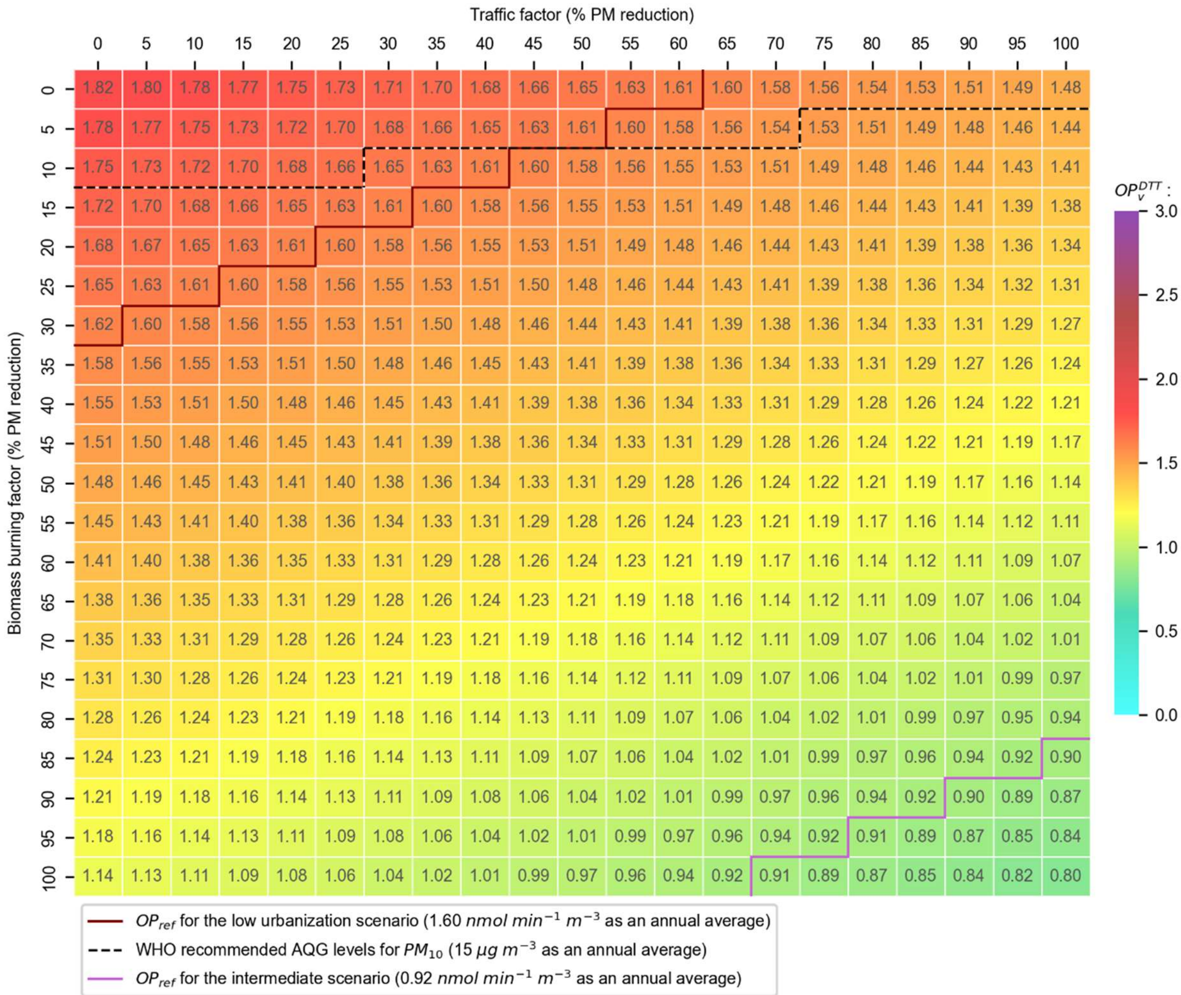


**Supplementary Figure 8| Matrix of $OP_v^{DTT}$ values based on the reduction of $PM_{10}$ from two sources (traffic and biomass burning factors) in the urban Alpine valley of CHAM (Chamonix, France).** The percentage reductions in traffic- and biomass-burning-related $PM_{10}$ refer to a one-year reference level based on average source contributions in Chamonix (2013–2014). Data gathered 115 samples collected between November 2013 and November 2014. The matrix was calculated using PMF and MLR results from Dinh Ngoc Thuy et al. (2024). The solid lines represent $OP_v^{DTT}$ reference values for the "low urbanization" scenario and the "intermediate" scenario. $OP_v^{DTT}$ reference values for the "low" and "very low anthropogenic pollution" scenarios ($\leq$ 0.80 nmolDTT min$^{-1}$ m$^{-3}$) are not shown because they are out of scale. The dashed line represents the WHO Air Quality Guidelines (AQG) level for $PM_{10}$ as an annual mean. The new regulatory threshold for $PM_{10}$ (20 µg m$^{-3}$) is not shown because it has already been reached in average for this site. The $OP_v^{DTT}$ levels (nmolDTT min$^{-1}$ m$^{-3}$) are going from low to high values with the colours changing from blue to violet.

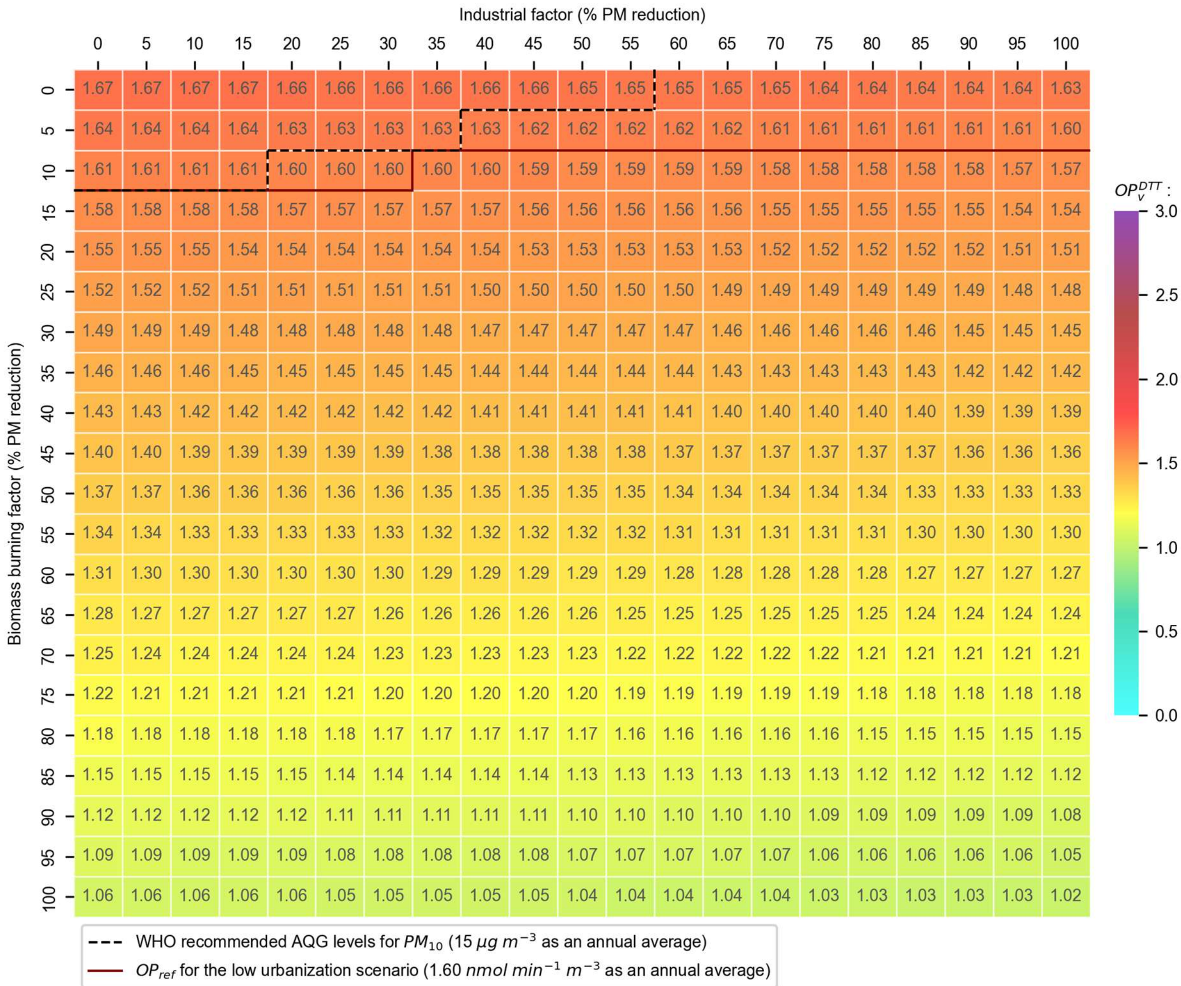


**Supplementary Figure 9| Matrix of $OP_v^{DTT}$ values based on the reduction of $PM_{10}$ from two sources (industrial and biomass burning factors) in the two industrial sites (Kanal in Slovenia and Port de Bouc in France).** The percentage reductions in industrial- and biomass-burning-related $PM_{10}$ refer to a multi-site, multi-year reference level based on average source contributions across the two studied sites (2014–2021). Data gathered 300 samples collected between November 2020 and November 2021 for Kanal and between June 2014 and June 2016 for Port de Bouc. The matrix was calculated using PMF and MLR results from Dinh Ngoc Thuy et al. (2024) and Glojek et al. (2024). The solid line represents $OP_v^{DTT}$ reference value for the "low urbanization" scenario. $OP_v^{DTT}$ reference values for the other scenarios (≤ 0.92 nmolDTT $min^{-1}$ $m^{-3}$) are not shown because they are out of scale. The dashed line represents the WHO Air Quality Guidelines (AQG) level for $PM_{10}$ as an annual mean. The new regulatory threshold for $PM_{10}$ (20 µg $m^{-3}$) is not shown because it has already been reached for in average these two sites. The $OP_v^{DTT}$ levels (nmolDTT $min^{-1}$ $m^{-3}$) are going from low to high values with the colours changing from blue to violet.

When looking at $OP_v^{AA}$ matrices, we observe that reducing biomass burning factor is a lot more efficient than reducing traffic factor for all site types, even the traffic site. For instance, in the valley site, it is possible to attain all the $OP_v^{AA}$ exposure scenarios by lowering the biomass burning factor alone. This is substantially different from the $OP_v^{DTT}$ matrix for the same site, for which only scenario 2 was achievable and required a considerable reduction in the two sources together. Similarly, almost any $OP_v^{AA}$ exposure scenario can be achieved by reducing $PM_{10}$ from biomass burning in the two combined industrial sites. However, a $PM_{10}$ reduction of at least 70% from the two sources is required to reach the "very low anthropogenic pollution" $OP_v^{AA}$ exposure scenario in rural areas, whereas all the scenarios were already achieved when $OP_v^{DTT}$ was considered instead. It is worth noting that regarding $PM_{10}$, $OP_v^{AA}$ reference values proved to be more restrictive than for $OP_v^{DTT}$. It is more difficult to achieve the $OP_{ref}$ in the following matrices. Yet for most types of sites, we can see that the high sensitivity of AA assay to the biomass burning source counterbalances the fact that the $OP_v^{AA}$ exposure scenarios are overall more restrictive than for $OP_v^{DTT}$.

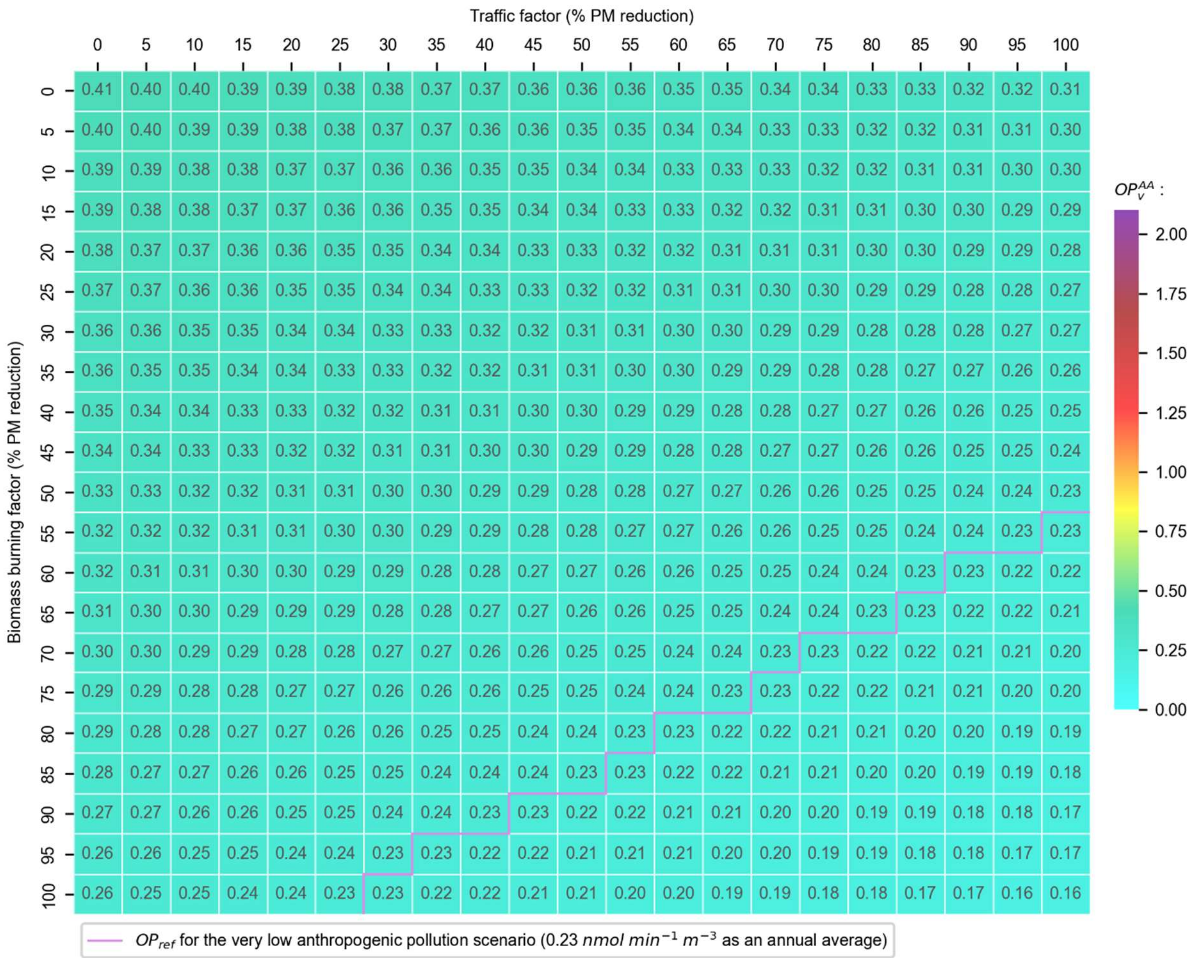


**Supplementary Figure 10| Matrix of $OP_v^{AA}$ values based on the reduction of $PM_{10}$ from two sources (traffic and biomass burning factors) in the rural site of OPE ("Observatoire Pérenne de l'Environnement", France).** The percentage reductions in traffic- and biomass-burning-related $PM_{10}$ refer to a multi-year reference level based on average source contributions in OPE (2012–2020). Data gathered 438 samples collected between March 2012 and December 2020. The matrix was calculated using PMF and MLR results from Borlaza et al. (2022). The solid line represents $OP_v^{AA}$ reference value for the "very low anthropogenic pollution" scenario. $OP_v^{AA}$ reference values for the other scenarios (≥ 0.60 nmolAA $min^{-1}$ $m^{-3}$) are not shown because they have already been reached in average for this site. Similarly, the WHO Air Quality Guidelines (AQG) level and the new regulatory threshold for $PM_{10}$ (respectively 15 and 20 µg $m^{-3}$) are not shown because have been achieved. The $OP_v^{AA}$ levels (nmolAA $min^{-1}$ $m^{-3}$) are going from low to high values with the colours changing from blue to violet.

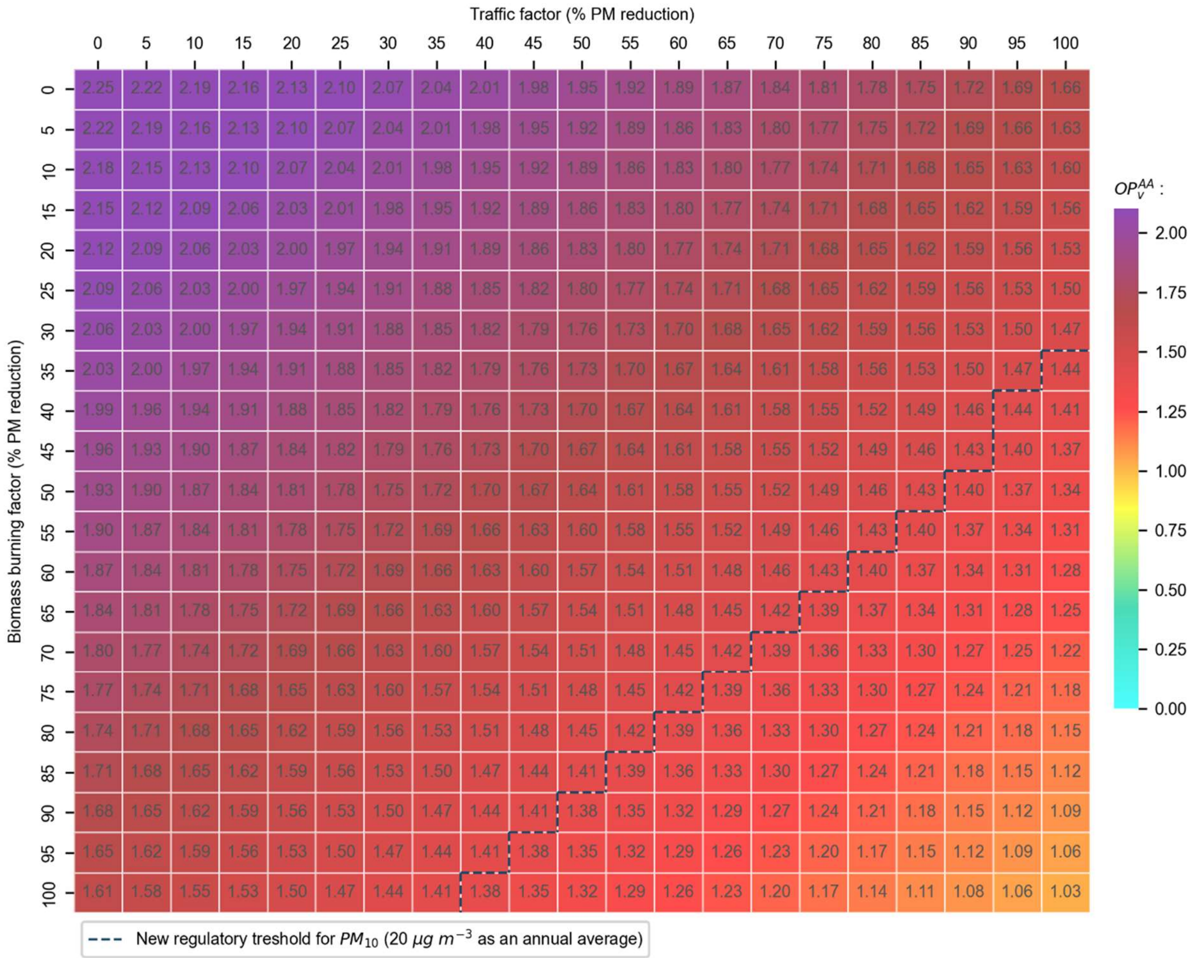


**Supplementary Figure 11| Matrix of $OP_v^{AA}$ values based on the reduction of $PM_{10}$ from two sources (traffic and biomass burning factors) in the traffic site of RBX (Roubaix, France).** The percentage reductions in traffic- and biomass-burning-related $PM_{10}$ refer to a one-year reference level based on average source contributions in Roubaix (2013–2014). Data gathered 156 samples collected between January 2013 and May 2014. The matrix was calculated using PMF and MLR results from Dinh Ngoc Thuy et al. (2024). The dashed line represents the new regulatory $PM_{10}$ threshold as an annual mean. The WHO Air Quality Guidelines (AQG) level for $PM_{10}$ (15 $\mu g\ m^{-3}$) is not shown because it cannot be reached in average for this site only with the reduction of these two sources (out of scale). Similarly, all $OP_v^{AA}$ reference values, even for the "low urbanization" scenario (0.99 nmolAA $min^{-1}\ m^{-3}$), are not shown because they are out of scale. The $OP_v^{AA}$ levels (nmolAA $min^{-1}\ m^{-3}$) are going from low to high values with the colours changing from blue to violet.

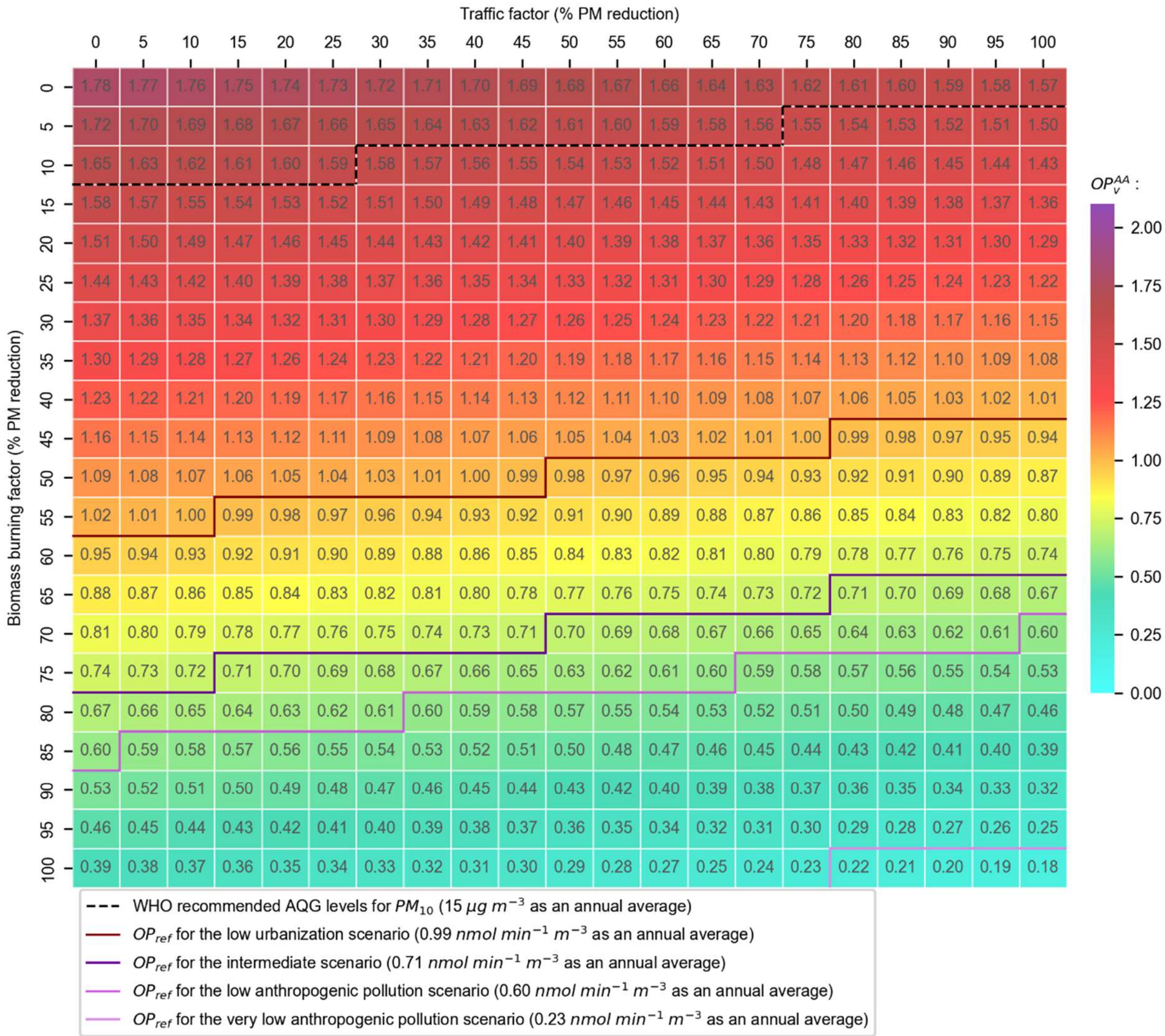


**Supplementary Figure 12| Matrix of $OP_v^{AA}$ values based on the reduction of $PM_{10}$ from two sources (traffic and biomass burning factors) in the urban Alpine valley of CHAM (Chamonix, France).** The percentage reductions in traffic- and biomass-burning-related $PM_{10}$ refer to a one-year reference level based on average source contributions in Chamonix (2013–2014). Data gathered 115 samples collected between November 2013 and November 2014. The matrix was calculated using PMF and MLR results from Dinh Ngoc Thuy et al. (2024). The solid lines represent $OP_v^{AA}$ reference values for all exposure scenarios. The dashed line represents the WHO Air Quality Guidelines (AQG) level for $PM_{10}$ as an annual mean. The new regulatory threshold for $PM_{10}$ (20 µg $m^{-3}$) is not shown because it has already been reached in average for this site. The $OP_v^{AA}$ levels (nmolAA $min^{-1}$ $m^{-3}$) are going from low to high values with the colours changing from blue to violet.

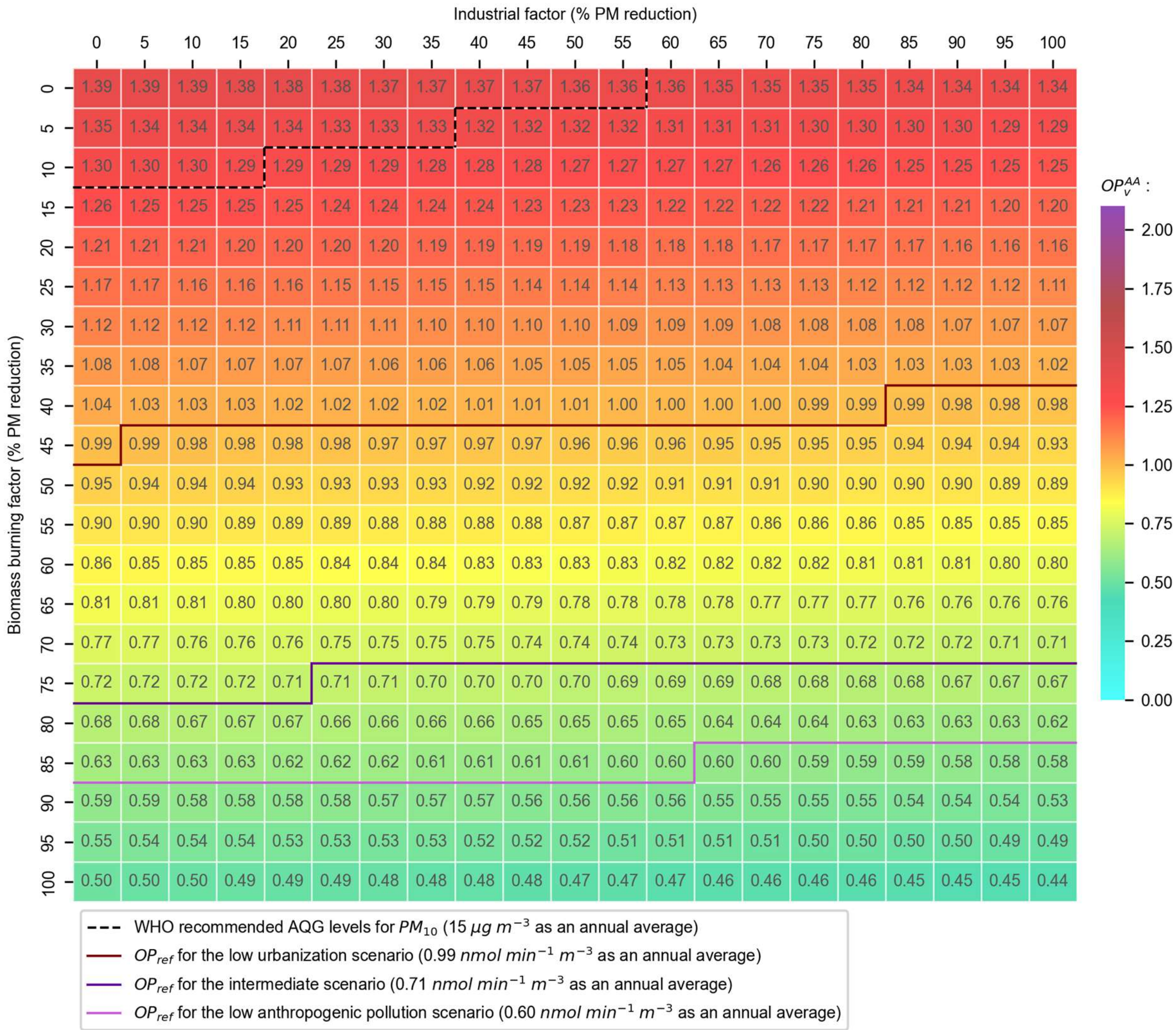


**Supplementary Figure 13| Matrix of $OP_v^{AA}$ values based on the reduction of $PM_{10}$ from two sources (industrial and biomass burning factors) in the two industrial sites (Kanal in Slovenia and Port de Bouc in France).** The percentage reductions in industrial- and biomass-burning-related $PM_{10}$ refer to a multi-site, multi-year reference level based on average source contributions across the two studied sites (2014–2021). Data gathered 300 samples collected between November 2020 and November 2021 for Kanal and between June 2014 and June 2016 for Port de Bouc. The matrix was calculated using PMF and MLR results from Dinh Ngoc Thuy et al. (2024) and Glojek et al. (2024). The solid lines represent $OP_v^{AA}$ reference values for the "low urbanization" scenario, the "intermediate" scenario and the "low anthropogenic pollution" scenario. $OP_v^{AA}$ reference value for the "very low anthropogenic pollution" scenario (0.23 nmolAA $min^{-1}$ $m^{-3}$) is not shown because it is out of scale. The dashed line represents the WHO Air Quality Guidelines (AQG) level for $PM_{10}$ as an annual mean. The new regulatory threshold for $PM_{10}$ (20 µg $m^{-3}$) is not shown because it has already been reached for in average these two sites. The $OP_v^{AA}$ levels (nmolAA $min^{-1}$ $m^{-3}$) are going from low to high values with the colours changing from blue to violet.

## S9. Validation of the linear regression models

Although the data for OP and PM mass concentration are not perfectly normally distributed, more consistent results were found when extreme values for each site type were excluded. Among the two analyses of the linear regression models, examining the residuals as a function of the predicted $OP_v$ values helped assess the linearity of the associations. The linear regression performed better for low $PM_{10}$ mass concentration values (below the $3^{rd}$ quartile), but errors increased at higher values. Indeed, all models showed an increase of data scatter with the predicted value, and more residuals below zero. Some standardized residuals fell outside of the satisfactory limits, especially for medium to high predicted values, indicating heterogeneity in the residuals' variance for these values. Overall, the models demonstrate better accuracy at lower theoretical values and became less reliable as PM concentrations increased. This suggested that $OP_v$ tends to be underestimated at higher PM mass concentration. Therefore, we chose to use robust linear regressions which need to be carefully interpreted and only help to visualize the influence of the local sources on OP (changes in slopes depending on the site type).

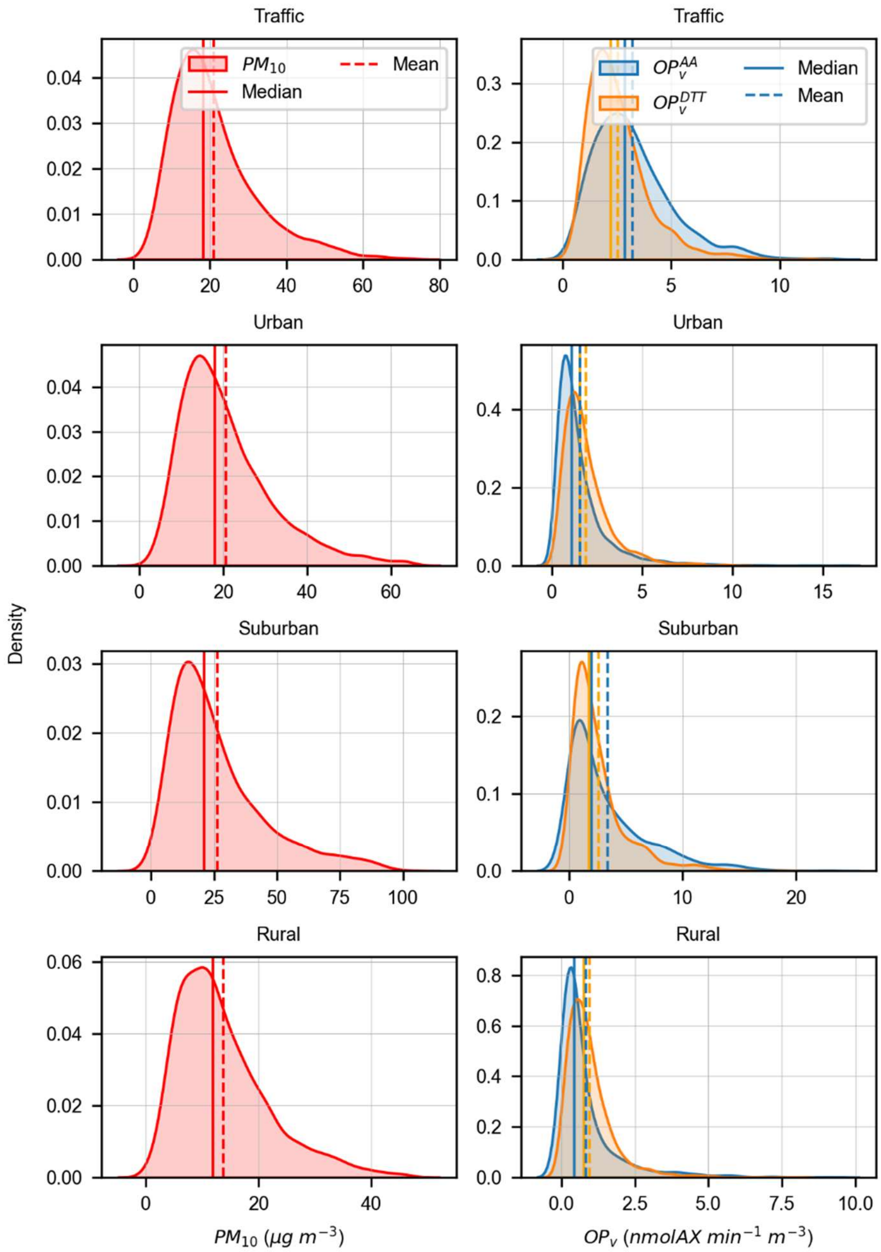


**Supplementary Figure 14| Distribution density of PM mass concentration (on the left) and $OP_v$ (on the right, AA assay in blue and DTT assay in orange) for $PM_{10}$ samples in the 4 site types selected.** Data without most of the sites with a valley topography (see Methods section). N=6,563 samples. The solid line represents the medians and the dotted line represents the mean. AX: Antioxidant (AA or DTT).

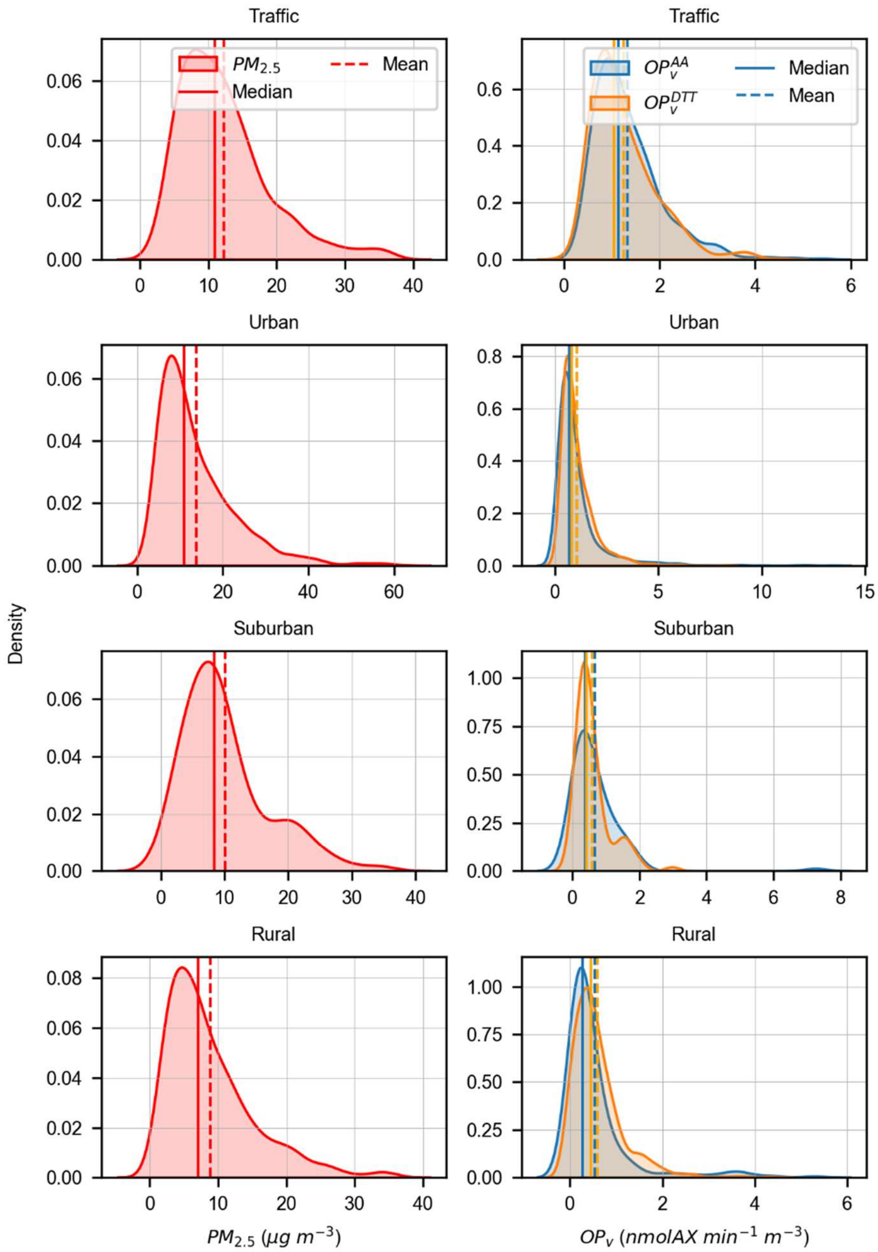


**Supplementary Figure 15| Distribution density of PM mass concentration (on the left) and $OP_v$ (on the right, AA assay in blue and DTT assay in orange) for $PM_{2.5}$ samples in the 4 site types selected.** Data without most of the sites with a valley topography (see Methods section). N=2,546 samples. The solid line represents the medians and the dotted line represents the mean. AX: Antioxidant (AA or DTT).

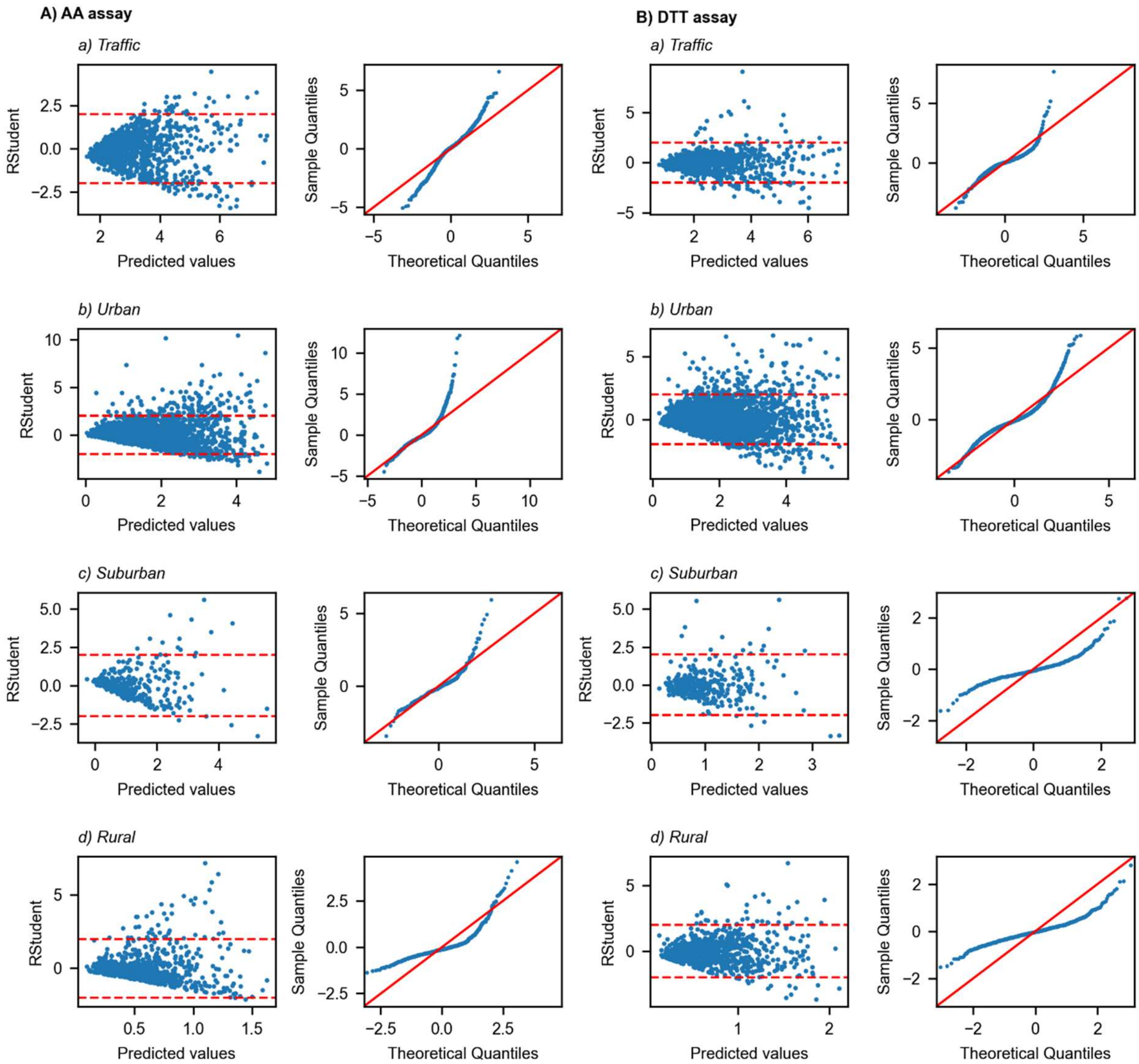


**Supplementary Figure 16| Analysis of the linear regression models between A) $OP_v^{AA}$ or B) $OP_v^{DTT}$ and PM mass concentration for $PM_{10}$ samples in the 4 site types selected.** Data without most of the sites with a valley topography (see Methods section). N=6,563 samples. Studentized residuals as a function of the $OP_v^{AA}$ values predicted by the linear regression model to assess the homogeneity of the variance of the residuals on the left. QQ plot (sample quantiles as a function of theoretical quantiles for a normal distribution) to assess the normality of the distribution of the residuals on the right. Unit: nmol $min^{-1}$ $m^{-3}$.

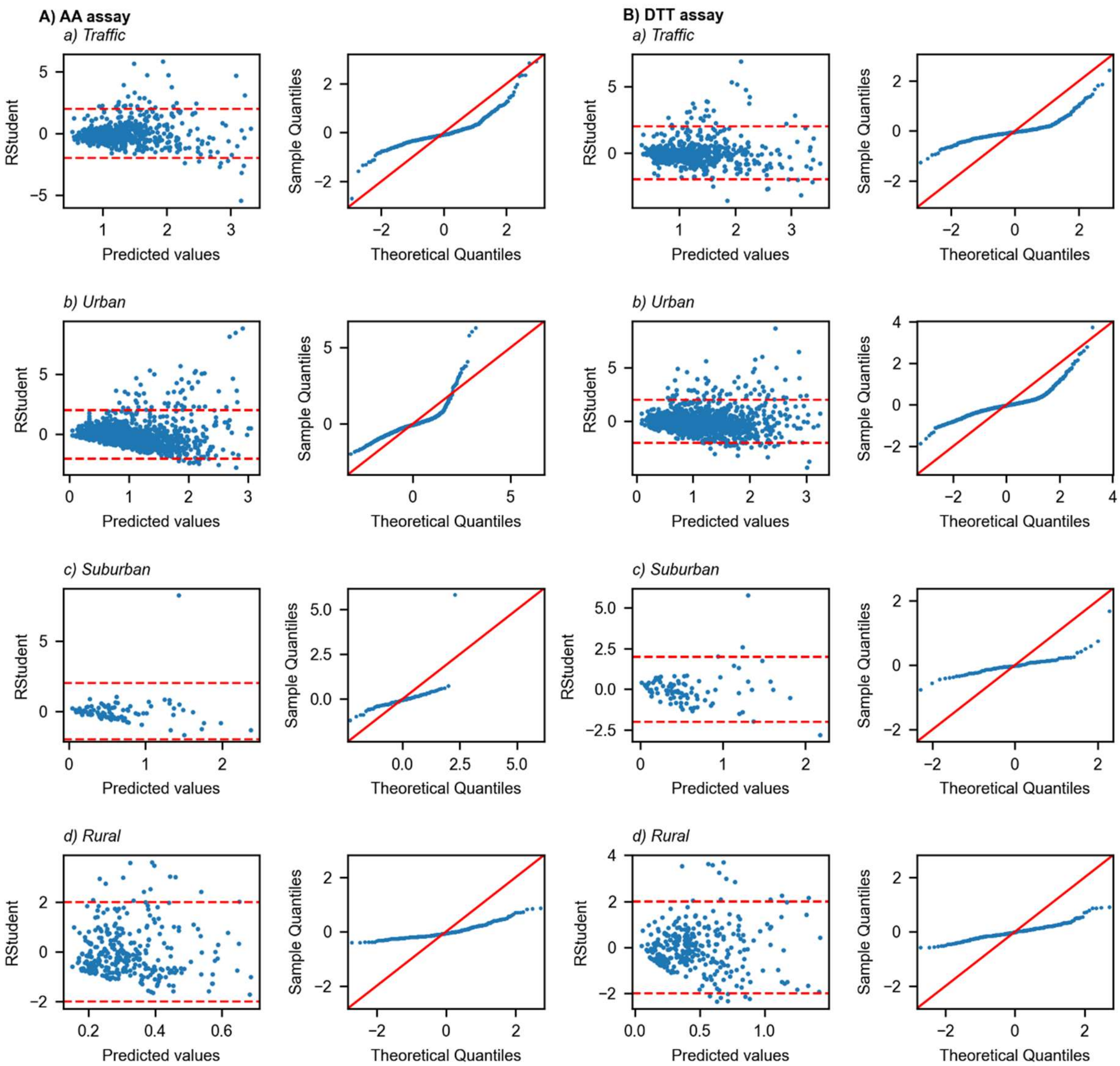


**Supplementary Figure 17| Analysis of the linear regression model between A) $OP_v^{AA}$ or B) $OP_v^{DTT}$ and PM mass concentration for $PM_{2.5}$ samples in the 4 site types selected.** Data without most of the sites with a valley topography (see Methods section). N=2,546 samples. Studentized residuals as a function of the $OP_v^{AA}$ values predicted by the linear regression model to assess the homogeneity of the variance of the residuals on the left. QQ plot (sample quantiles as a function of theoretical quantiles for a normal distribution) to assess the normality of the distribution of the residuals on the right. Unit: nmol $min^{-1}$ $m^{-3}$.

## S10. Mass normalization bias in OP responses

Charrier et al. (2016) found that the $OP_m^{DTT}$ response was biased by the PM mass concentration used for the extraction in case of high contributions from Cu and Mn. However, some samples of our database were extracted with a PM mass concentration of 10 µg $mL^{-1}$ while many were extracted at 25 µg $mL^{-1}$. This could lead to a bias in $OP^{DTT}$ measurements and make difficult the comparison between sites. To check if this bias was significant at large scale, we observed the distribution of $PM_{10}$ OP from the samples extracted in both mass concentration at a time (10 µg $mL^{-1}$ and 25 µg $mL^{-1}$ – approximatively 4% of the samples in the database) as a function of $PM_{10}$ mass concentration in the air (µg $m^{-3}$). These distributions were evaluated thanks to KDE plots (Kernel Density Estimate plots) allowing to visualize the distribution of observations in multiple dimensions using continuous probability density curve. It appears that these disparities in the extraction concentrations did not affect much the $OP_m^{AA}$ results but $OP_m^{DTT}$ seems to be a little overestimated for approximately ¼ of the $PM_{10}$ samples at 10 µg $mL^{-1}$ compared to the others. It is worth noting that for the data with both extraction concentrations, we finally kept only the OP values at 25 µg $mL^{-1}$. Thus, with such a high scale we considered that this bias was negligible especially since 86% of the database has data at 25 µg $mL^{-1}$.

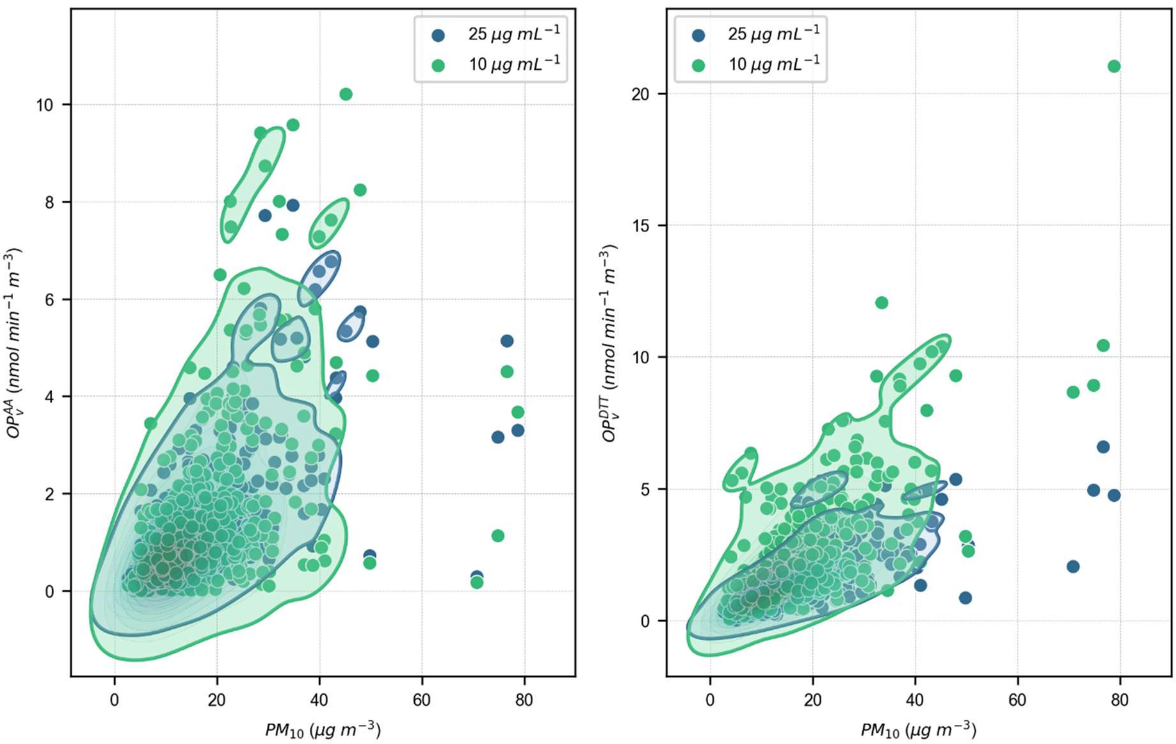


**Supplementary Figure 18| Scatter plot and KDE (Kernel Density Estimation) plot of $OP_v$ as a function of PM mass concentration for $PM_{10}$ samples extracted with both final concentration of 10 µg $ml^{-1}$ (green dots) and 25 µg $ml^{-1}$ (blue dots).** N=465 samples.

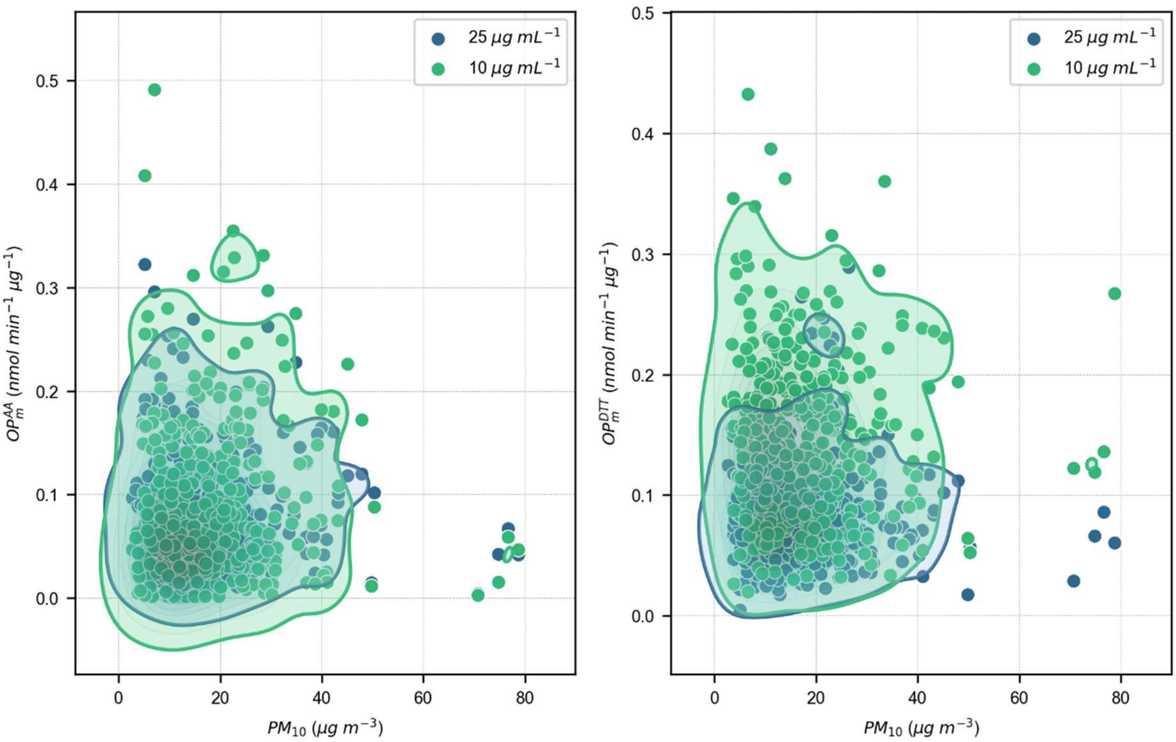


**Supplementary Figure 19| Scatter plot and KDE (Kernel Density Estimation) plot of $OP_m$ as a function of PM mass concentration for $PM_{10}$ samples extracted with both final concentration of 10 µg $ml^{-1}$ (green dots) and 25 µg $ml^{-1}$ (blue dots).** N=465 samples.

## S11. References


Salana, S. et al. Inter-continental variability in the relationship of oxidative potential and cytotoxicity with PM2.5 mass. *Nat. Commun*. **15**, 5263 (2024).

Font, A. et al. Long–term measurements of aerosol composition at rural background sites in France: sources, seasonality and mass closure of PM2.5. *Atmos. Envir*., **334**, 120724. (2024).

Borlaza, L. J. et al. Nine-year trends of PM10 sources and oxidative potential in a rural background site in France. *Atmospheric Chem. Phys*. **22**, 8701–8723 (2022).

Ngoc Thuy Dinh, V. et al. Decadal trends (2013–2023) in PM10 sources and oxidative potential at a European urban supersite (Alpine Valley, Grenoble, France), *EGUsphere* [preprint], (2025).

C.A. Belis et al. Sources for PM air pollution in the Po Plain, Italy: I. Critical comparison of methods for estimating biomass burning contributions to benzo(a)pyrene. *Atmos. Environ*. **45** (2011).

Weber, S. et al. Comparison of PM10 Sources Profiles at 15 French Sites Using a Harmonized Constrained Positive Matrix Factorization Approach. *Atmosphere* **10**, 310 (2019).

Glojek, K. et al. Annual variation of source contributions to PM10 and oxidative potential in a mountainous area with traffic, biomass burning, cement-plant and biogenic influences. *Environ. Int.* **189**, 108787 (2024).

Norris, G., Duvall, R., Brown, S. & Bai, S. EPA Positive Matrix Factorization (PMF) 5.0 Fundamentals and User Guide. (2014).

Belis, C.A. et al. European guide on air pollution source apportionment with receptor models - Revised version 2019, EUR 29816 EN, *Publications Office of the European Union*, Luxembourg. (2019).

Bates, J. T. et al. Reactive Oxygen Species Generation Linked to Sources of Atmospheric Particulate Matter and Cardiorespiratory Effects. *Environ. Sci. Technol*. **49**, 13605–13612 (2015).

Dinh Ngoc Thuy, V. et al. Unveiling the optimal regression model for source apportionment of the oxidative potential of PM. *Atmospheric Chem. Phys.* **24** 7261-7282 (2024).